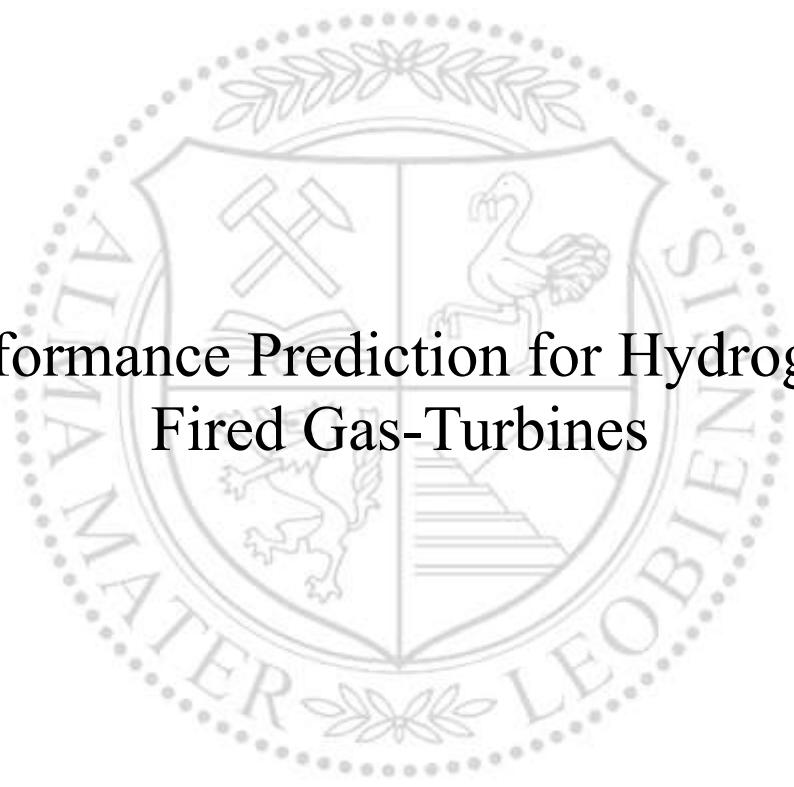




Chair of Energy Network Technology

Master's Thesis



Performance Prediction for Hydrogen-
Fired Gas-Turbines

Philipp Gradl, BSc

October 2022



AFFIDAVIT

I declare on oath that I wrote this thesis independently, did not use other than the specified sources and aids, and did not otherwise use any unauthorized aids.

I declare that I have read, understood, and complied with the guidelines of the senate of the Montanuniversität Leoben for "Good Scientific Practice".

Furthermore, I declare that the electronic and printed version of the submitted thesis are identical, both, formally and with regard to content.

Date 24.10.2022

Signature Author
Philipp Gradl

Abstract

This work aims to predict if the gas turbine SGT-800 (57 MW) can cope with a fuel change from methane to hydrogen. Therefore a physical simulation model of this gas turbine is created in Epsilon Professional. This physical simulation model is reverse engineered from the correction curve model of the SGT-800 (57 MW) in Epsilon Professional. Reverse engineering is subdivided into four major steps. The first one is the creation of the physical simulation model. In this step, the gas turbine SGT-800 (57 MW) gets modeled as closely as possible. Some of the parameters in this model are set by regressions. The second step is the so-called Reference Run. This step aims to generate data for fitting the regressions used in the physical simulation model. Since the regressions are not fitted at this stage, the physical simulation models take these values from the correction curve model. At this point, the physical simulation model cannot make stand-alone calculations. After the needed data is generated, the regressions used in the physical simulation model are fitted. With these fitted regressions, the model can make stand-alone predictions. The third step is the Validation Run. The Validation Run aims to see if the physical model can predict close enough results compared to the correction curve model. After this is true, it is assumed that the physical simulation model can properly model the behavior of the gas turbine SGT-800 (57 MW). In the last step of the so-called Hydrogen Run, the fuel changes from methane to hydrogen. The results of this Hydrogen Run show that the fuel system tends to use too much fuel. The reason for this is a change in the expansion behavior of the flue gas. This additional fuel consumption results in a higher turbine power generation of about 2 MW. It also causes a rise in the firing temperature. This rise in the firing temperature can cause damage to the turbine. This thesis concludes that the fuel control system has to be adapted if the fuel gets changed from methane to hydrogen.

Contents

Abstract	I
Contents	II
Nomenclature	IV
List of figures	VI
1. Introduction	1
2. Task assignments	3
3. Theoretical introduction to gas turbines	6
3.1 Joule Cycle.....	7
3.1.1 1-2 Isentropic compression	7
3.1.2 2-3 Isobaric heat supply	8
3.1.3 3-4 Isentropic expansion	8
3.1.4 4-1 Isobaric dissipation.....	8
3.2 Cycle efficiency	9
4. Gas turbine parameters	11
4.1 Basics of dimensional analysis	11
4.2 Important performance parameters of a gas turbine	15
4.2.1 The Mach number	15
4.2.2 The normalized corrected mass flow	20
4.2.3 The normalized corrected speed	24
4.3 Performance maps.....	27
4.3.1 Compressor map	27
4.3.2 Turbine map	28
5. Creating a simulation model	29
5.1 The Correction Curve Model.....	29
5.2 Reverse engineering the physical model	30
5.2.1 Modeling concept of the compressor	31

5.2.2	Modeling the compressor in Ebsilon Professional	32
5.2.3	Modeling concept of the combustion system	34
5.2.4	Modeling the combustion system in Ebsilon Professional	35
5.2.5	Modeling concept of the turbine	35
5.2.6	Modeling of the turbine in Ebsilon Professional	36
5.2.7	Modeling concept of the mechanical losses	39
5.2.8	Modeling of the mechanical losses in Ebsilon Professional	39
5.2.9	The complete gas turbine model in Ebsilon Professional	40
5.3	Design and Off-design calculation	41
5.4	Calculation of the Reference Run	48
5.4.1	Multivariant polynomial regressions	48
5.4.2	Multivariant polynomial regression of the compressor	49
5.4.3	Defining a multivariant polynomial regression for the combustion	52
5.4.4	Narrowing down the combustion regression	55
1.1.1	Defining a multivariant polynomial regression for the turbine	56
5.4.5	Defining a multivariant polynomial regression for the losses	60
5.5	Calculation of the Validation Run	62
5.5.1	Validation of the air mass flow	63
5.5.2	Validation of the fuel power flow	64
5.5.3	Validation of the isentropic turbine efficiency	65
5.5.4	Validation of the generated power	65
5.6	Calculation of the Hydrogen Run	66
5.6.1	Air mass flow in the compressor	67
5.6.2	Exhaust temperature	67
5.6.3	Generated electrical power	68
6.	Result discussion	70
7.	Conclusion	76
8.	Bibliography	77

Nomenclature

NCSPD	Normalized Corrected Speed
NCFLW	Normalized Corrected Flow
EXPR	Expansion Ratio
η_{is}	Isentropic Efficiency
η_{th}	Thermal Efficiency
c_p	Specific Heat Capacity
\dot{m}	Mass Flow
T	Temperature
p	Pressure
\dot{Q}	Heat Flow
\dot{W}	Power
ρ	Density
V	Volume
h	Height
g	Gravitational Acceleration
E_{pot}	Potential Energy
Ma	Mach Number
c	Speed of Sound
u	Flow Speed
v	Specific Volume
A	Flow Area
P	Power
γ	Isentropic Exponent

Nomenclature

D	Flow Diameter
R_s	Molar Gas Constant
Ω	Rotational Speed
H	Enthalpy

List of figures

2-1: Outline of the Reference Run	4
2-2: Outline of the Validation Run	4
2-3: Outline of the Hydrogen Run	5
3-1: Outline structure of a gas turbine [13]	6
3-2: T-S diagram of a Joule Cycle.....	7
4-1: Example of a compressor map inspired by [28]	27
4-2: Example of a turbine map inspired by [28].....	28
5-1: Schematic function of the compressor model.....	31
5-2: Part of the modeled compressor	32
5-3: Compressor Efficiency for Base Load Operation	33
5-4: Schematic function of the combustion system	34
5-5: Combustion system in Epsilon Professional	35
5-6: Schematic function of a turbine.....	36
5-7: Implementation of the turbine	37
5-8: Implementation of a turbine stage	37
5-9: Ideal expansion compared to real expansion	38
5-10: Schematic function of the loss block	39
5-11: Implementation of the loss map in Epsilon Professional	40
5-12: All blocks combined to turbine model.....	40
5-13: Operating space of the turbine model.....	42
5-14: Comparison of distributions	43
5-15: Distribution of the used ambient temperature values.....	44
5-16: Distribution of the used ambient pressure values	45
5-17: Distribution of the used ambient humidity values	45
5-18: Representation of the correlation between the ambient pressure and temperature ..	46
5-19: Representation of the correlation between the ambient temperature and humidity ..	47
5-20: Representation of the correlation between the ambient humidity and pressure.....	47
5-21: Graphical representation of all terms for a multivariant regression with three input parameters.....	49
5-22: Air mass flow for multiple scenarios.....	51
5-23: Validation of the air mass flow	52
5-24: Operating space of the fuel system regression	54

5-25: Validation of the exhaust temperature	55
5-26: Operating area of the regression	56
5-27: Representation of all used regressions.....	58
5-28: All used regressions and the interval borders	59
5-29: Prediction error of the used regression.....	59
5-30: Operating space of the loss map	61
5-31: Validation of the air mass flow for new scenarios.....	63
5-32: Validation of the fuel power flow for new scenarios	64
5-33: Plot of the exhaust temperature	65
5-34: Validation of the power generation for new scenarios.....	66
5-35: Comparison of the air mass flow	67
5-36: Comparison of the exhaust temperatures.....	68
5-37: Comparison of the generated power.....	68
6-1: Isentropic turbine efficiencies for methane and hydrogen	70
6-2: Heat rates for both runs.....	71
6-3: Compression Ratio Comparison.....	72
6-4: Comparison of the fuel consumption	72
6-5: Comparison of the isentropic power for different fuels.....	73
6-6: Comparison of the generated power for different fuels	74
6-7: Comparison between the isentropic power and the generated power for different fuels	74
6-8: Firing temperature for different fuels	75

1. Introduction

Climate change is an issue that has become increasingly important. One of the main causes of global warming is the extensive emission of greenhouse gases. One of the most prominent greenhouse gases is CO₂. To cope with this problem, the EU aims to reduce CO₂ emissions by 55 percent by 2030 and by another 45 percent by 2050 [1]. One part of the solution is to build more renewable power plants. In 2020, only 21.3 percent of the overall EU energy consumption came from renewable energies [2]. The objective is to achieve a share of more than 90 percent in 2050 [2]. This mandatory increase in renewable power plants, however, comes at a price as it creates challenges to stabilize the power grid. This is so because renewable power plants like wind and solar power plants depend on ambient conditions. Since the frequency of the power grid changes when power generation and consumption are not balanced, the imprecise predictability of renewable power generation can lead to instability. This problem will be increasingly dominant with the rising share of these plants in the future.

Gas turbines could solve this problem because they are well suited for this task for several reasons. On the one hand gas turbines can generate large amounts of power, up to hundreds of megawatts [3, 4]. On the other hand they can greatly vary the power generated depending on the operating point of the turbine, which can be changed rapidly. For some gas turbines the ramp rate is in the tens of MW [5]. Therefore these power plants could help keep the power grid frequency at a reasonable level [6].

So far, there is an important drawback, however. Gas turbines often use methane as fuel and therefore they emit CO₂. This problem could be eliminated if hydrogen could be used instead. Other than methane, hydrogen does not create any CO₂ when being combusted. Therefore a hydrogen-fueled gas turbine would operate without emitting any CO₂.

Another interesting aspect for using hydrogen with a gas turbine is that hydrogen is often considered a chemical storage compound in power-to-gas plants [7]. Such power-to-gas plants use excess electricity to generate hydrogen, which then can then be stored. If energy is needed gas turbines could use this hydrogen for power generation. Even if the gas turbine is not powered exclusively by hydrogen, it could be added to the natural gas and reduce the consumption of natural gas and therefore the emission of CO₂. Step by step, the percentage of hydrogen mixed with the natural gas could be increased to reduce the need for natural gas over time.

An alternative technology for using the generated hydrogen are fuel cells. Fuel cells are often considered for converting hydrogen into electric energy, but most fuel cells have a nominal power below 2.8 MW [8]. In comparison, a single gas turbine can generate hundreds of megawatts of power [3]. These technologies operate on a different power scale.

Due to the high pressure ratio, gas turbines can reach incredibly high efficiencies. If the turbines high temperature exhaust gases are used in a steam turbine, the whole cycle can reach an electric efficiency above 62 percent [9]. Another aspect that favors the idea of hydrogen-powered gas turbines is it that these plants already exist and no new construction work would be needed. There are currently around 1007 operational gas power plants in Europe [10]. The only cost incurred would be the result of the fuel switch from methane to hydrogen.

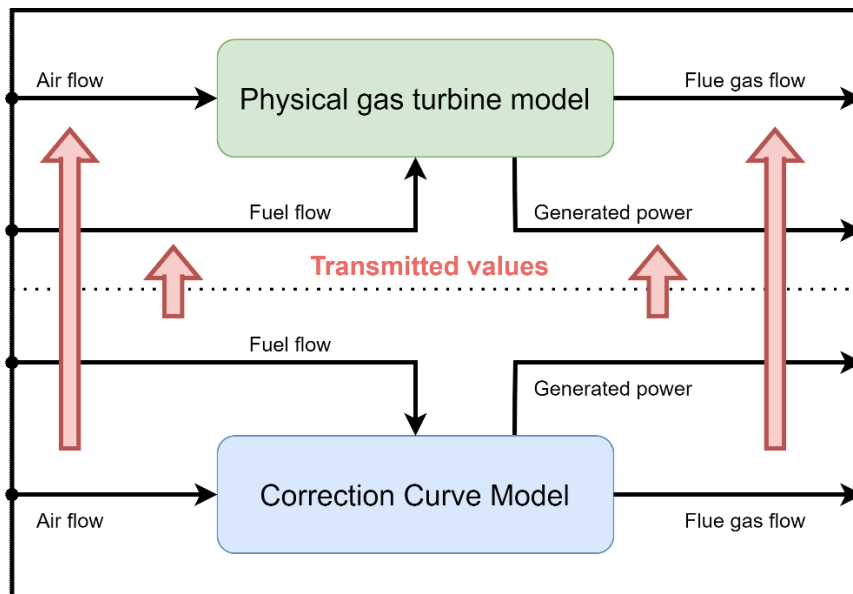
All these advantages show that gas turbines could play an essential role in the energy transition. Since there are currently numerous operational gas turbines fueled by natural gas, it is essential to know if they could also be powered by hydrogen. If so, they could be a viable option for using the produced hydrogen. The objective of this thesis is to create a simulation model of the gas turbine SGT-800 (57 MW) that can predict the behavior of this gas turbine when fueled with hydrogen. This behavioral change is then analyzed to see whether this gas turbine could cope with the fuel change.

2. Task assignments

This thesis aims to establish whether it is theoretically possible to power existing gas turbines with hydrogen. Currently, there are only correction curve models of gas turbines available, because the engine simulations are often proprietary [11]. These correction curve models only mimic the behavior of the gas turbines they are based on. They work by applying a set of different correction factors to reference values based on ambient conditions. [12] Therefore they cannot predict how a gas turbine's behavior would change if the fuel were changed from methane to hydrogen. One possible solution to this problem is a physical simulation of a gas turbine. This model can calculate the impact of fuel changes on the turbine. Therefore it does not rely on predefined correction curves.

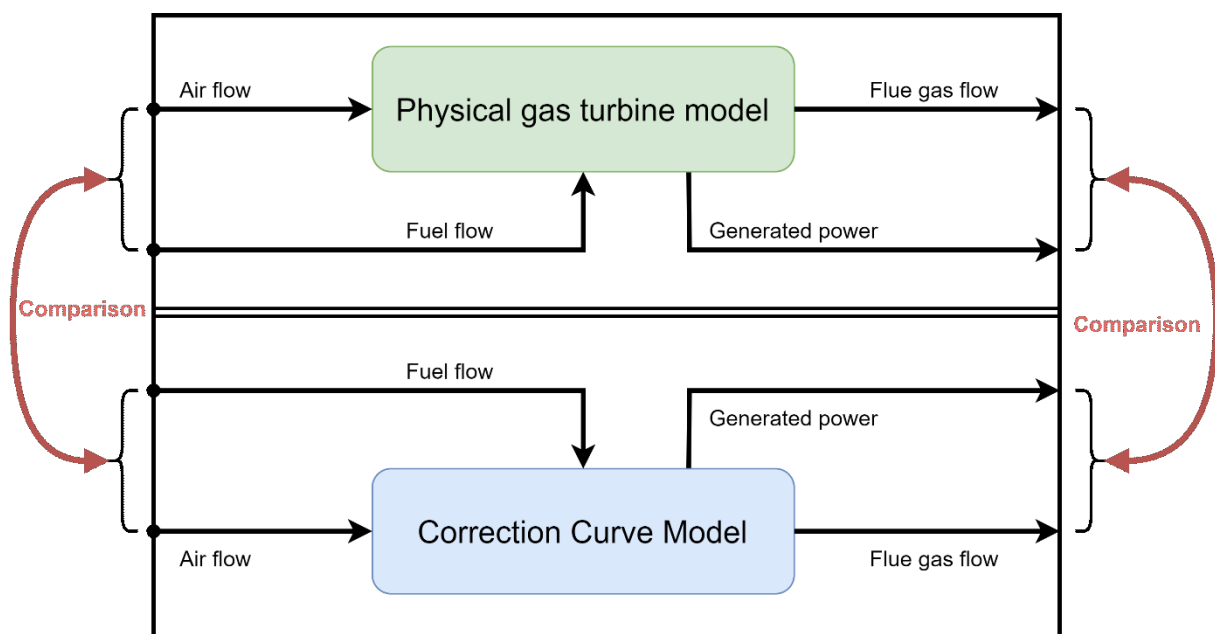
This thesis uses the SGT-800 (57 MW) gas turbine as example and creates a physical simulation model for predicting the turbine's behavioral change if the fuel switches from methane to hydrogen. This model will be reverse engineered from existing data. The simulation model is then used to analyze how the SGT-800 (57 MW) gas turbine would perform if it were fueled with hydrogen. In the following, a broad overview of the content of this thesis is given.

This thesis will describe the process of creating a physical simulation model in seven Chapters. Chapter 3 gives a basic introduction to gas turbine components and the ideal gas turbine cycle. Chapter 4 describes the mathematical origin of important gas turbine performance indicators like the mach number, the normalized corrected speed, and the normalized corrected mass flow. It also shows common representations of these performance indicators like the compressor and turbine map. Chapter 5.1 explains the process of creating the gas turbine simulation model. The Chapters 5.2 to 5.2.9 give a more detailed look at the correction curve model and the implementation of the simulation model in Epsilon Professional. It also explains that some parameters are going to be predicted by regressions. These regressions are going to be fitted in Chapter 5.4. In order to generate data for these regressions to fit, the correction curve model is used as a reference for the physical simulation model. Therefore the physical model uses the air mass flow, the fuel mass flow, the generated power and the flue gas exhaust temperature of the correction curve model to calculate multiple scenarios. This run is also referred as Reference Run. The following (2-1) diagram is a graphical representation of the Reference Run. The red arrows show the transmitted values from the correction curve model to the physical model.



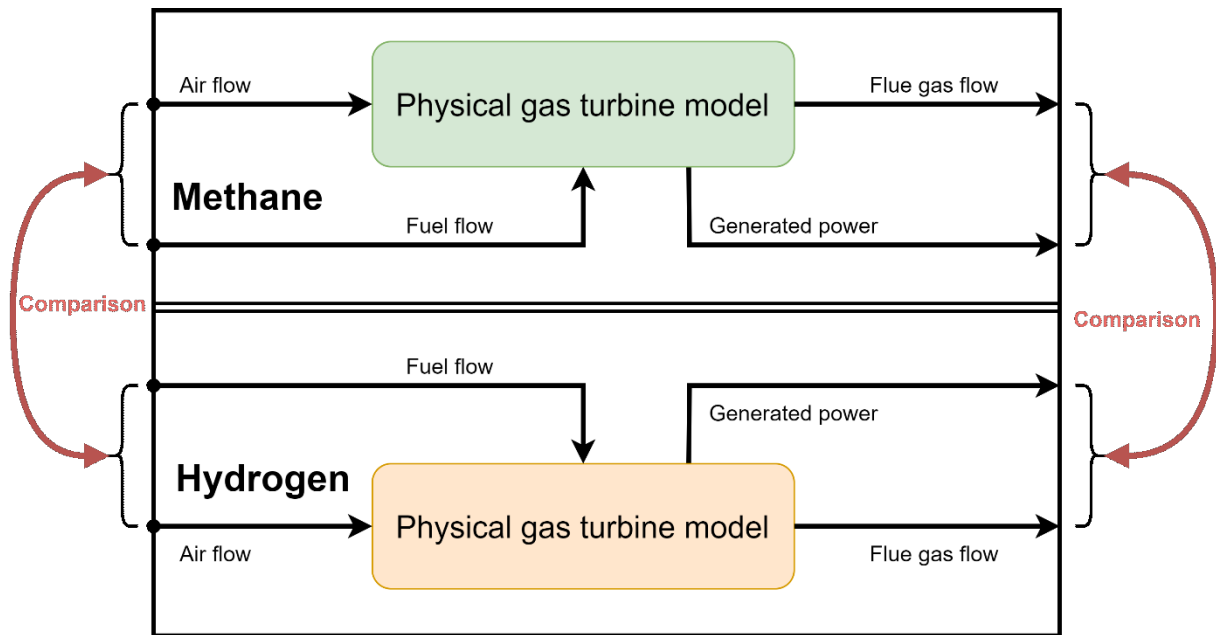
2-1: Outline of the Reference Run

This approach is necessary because the regressions use parameters that are not available in the correction curve model. After all, regressions are fitted, the Validation Run is explained and executed in Chapter 5.5. In this run, both models work independently and no values are transmitted from the correction curve model to the physical model. This is shown in the diagram of the Validation Run (2-2). The aim of this run is to see if all regressions works as expected and produce accurate results. This run is also calculated for multiple scenarios.



2-2: Outline of the Validation Run

The deviations in the results for these two models are also shown in Chapter 5.5. In the last step, the fuel is switched from methane to hydrogen in Chapter 5.6. This is done without making any other change in the model.

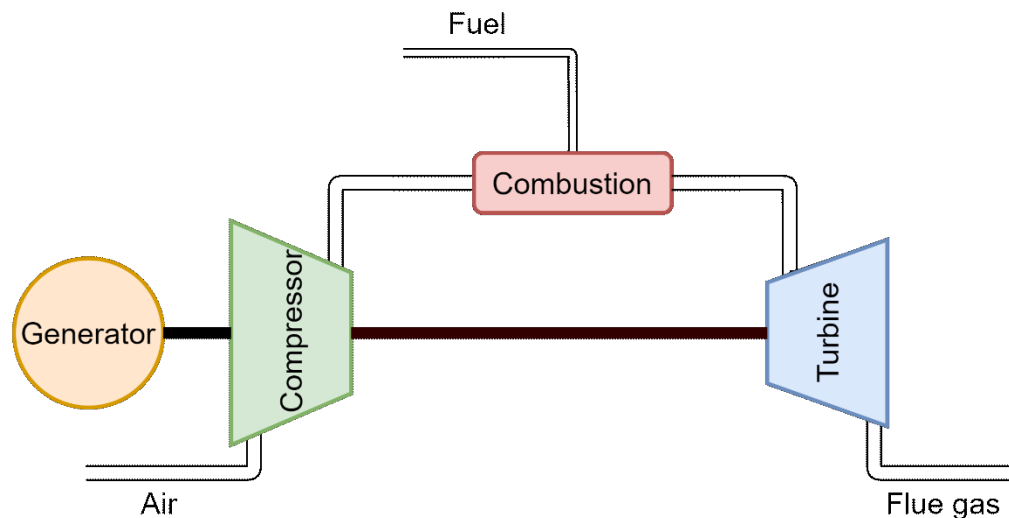


2-3: Outline of the Hydrogen Run

This setup is calculated for the same scenarios as the Validation Run. In Chapter 6, the results of the Hydrogen Run in Chapter 5.6 gets analyzed and interpreted. This thesis ends with the conclusion in Chapter 7.

3. Theoretical introduction to gas turbines

A gas turbine consists of four main components. These components are the compressor, the combustion chamber, the turbine, and the generator. The schematic structure of a gas turbine can be seen in the following figure.



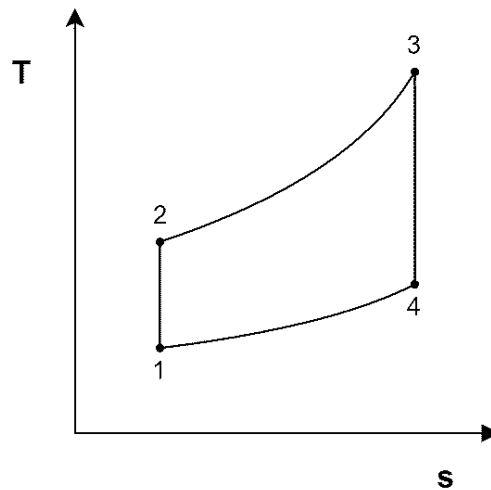
3-1: Outline structure of a gas turbine [13]

The compressor functions as air intake and compresses the aspired air to the pressure level needed. Due to practical limitations, a compressor consists of multiple stages. Each stage has a rotor and a stator. [13] After the air exits the compressor at the required pressure level, it reaches the combustion chamber, where the fuel gets burned. The so-produced flue gas has a much higher temperature than the air at the inlet of the combustion chamber. At this point, the flue gas has reached its highest pressure and temperature level. After the flue gas leaves the combustion chamber, it flows to the inlet of the turbine. The flue gas expands to a lower pressure and temperature level at the turbine. The flue gas's outlet temperature and pressure are lower, resulting in a lower enthalpy. [14]

The turbine itself can also consist of multiple stages due to practical limitations. Therefore, it can have multiple rows of rotors. Each of these rotor rows transfers a part of the enthalpy in the flue gas to the turbine shaft. [15] Some of this energy is used to power the compressor, which sits on the same shaft as the turbine, which is why the turbine needs to supply more power than the compressor consumes to work. Usually, the turbine produces significantly more power than the compressor's demand. With this excess power, it is possible to generate electric energy. [14] The ideal process behind the gas turbine is the so-called joule cycle. The joule cycle will be explained in detail in the next chapter.

3.1 Joule Cycle

The performance of an ideal gas turbine is described by the joule cycle [16]. With this ideal process, it is possible to calculate the highest possible efficiency and specific power output for a gas turbine considering limitations like maximum temperature and pressure level [13]. The comparison with the joule cycle makes it possible to estimate the compressor's and turbine's efficiency. As shown in the following diagram this cycle consist of four steps [17].



3-2: T-S diagram of a Joule Cycle

Each of these cycle steps also represents a task for a component in the turbine. [17] Therefore each of these steps is explained in further detail in the following. In contrast to an actual gas turbine, the joule cycle assumes that the fluid's composition and mass flow stays the same [18].

3.1.1 1-2 Isentropic compression

In this step, the fluid gets isentropically compressed to the pressure level needed. Therefore, the entropy change is zero. In reality, there would be a slight increase in entropy. The power consumption of an ideal compression is calculated with the formula (3-1). In this formula, W_{12} is the compressor's power consumption, \dot{m} is the air mass flow in the compressor, c_p is the specific heat capacity of air, T_1 is the air's inlet temperature, and T_2 is the exit temperature of the air. [19]

$$W_{12} = \dot{m} \cdot c_p \cdot (T_2 - T_1) \quad (3-1)$$

Since the power delivered in the system is considered positive, the power required to compress this mass flow has to be positive. In the case of a gas turbine, this step represents the compressor's compression of the aspired air.

3.1.2 2-3 Isobaric heat supply

As a result of the isobaric heat supply, the fluid reaches a higher temperature level. In the case of a gas turbine, the heat comes from the combustion of natural gas. In literature the firing temperature ranges from 1300 °C – 1600 °C [20, 21]. Even though the temperature rises, the pressure stays the same. Therefore, it has the same pressure level as the outlet of the compressor. The amount of heat supplied to the process can be calculated with the formula (3-2). In this formula, Q_{23} represents the supplied heat, T_2 is the inlet temperature, and T_3 is the exit temperature. [19]

$$\dot{Q}_{23} = \dot{m} \cdot c_p \cdot (T_3 - T_2) \quad (3-2)$$

This formula is only valid for the ideal process because, in reality, the combustion of the fuel would change the composition of the gas and the mass flow.

3.1.3 3-4 Isentropic expansion

By the isentropic expansion, the fluid expands from a higher pressure and temperature level to a lower one. Therefore, the turbine's rotors use this gas expansion to create rotational energy. Many turbines have multiple rotors to convert the kinetic energy of the fluid into rotational energy. This rotational energy is then transferred to the turbine shaft.

The so-generated power can be calculated with the formula (3-3). In this formula, W_{34} is the generated power, c_p is the specific heat capacity of the gas, T_3 is the inlet temperature in the turbine, and T_4 is the exit temperature. [22]

$$\dot{W}_{34} = \dot{m} \cdot c_p \cdot (T_3 - T_4) \quad (3-3)$$

This formula is only valid for the ideal process. In reality, the mass flow and the composition of the gas through the turbine can change due to bleed flows.

3.1.4 4-1 Isobaric dissipation

The gas must be cooled to the starting temperature to close the cycle. Most gas turbine have an open joule cycle [23]. Therefore, this last step is not realized. The only reason for cooling down the flue gas is to use the waste heat, but the flue gas does not get compressed again. The dissipated heat can be calculated with the formula (3-4) [22].

$$\dot{Q}_{41} = \dot{m} \cdot c_p \cdot (T_1 - T_4) \quad (3-4)$$

All these processes combined represent the joule cycle. This joule cycle is beneficial in predicting the highest possible efficiency. This ideal cycle can be used as a reference for actual gas turbines.

3.2 Cycle efficiency

If all of these formulas are combined, it is possible to calculate the highest possible efficiency for this cycle. Since power leaving the system is stated with a negative sign, it is necessary to change the sign convention. The resulting formula calculates the generated power by subtracting the compressor's power consumption from the turbine's power generation. [19, 22]

$$\Delta\dot{W}_{ls} = (-\dot{W}_{34}) - \dot{W}_{12} \quad (3-5)$$

$$\Delta\dot{W}_{ls} = -\left(\dot{m} \cdot c_p \cdot (T_4 - T_3)\right) - \dot{m} \cdot c_p \cdot (T_2 - T_1) \quad (3-6)$$

$$\Delta\dot{W}_{ls} = \dot{m} \cdot c_p \cdot (T_3 - T_4) - \dot{m} \cdot c_p \cdot (T_2 - T_1) \quad (3-7)$$

$$\Delta\dot{W}_{ls} = \dot{m} \cdot c_p \cdot (T_3 + T_1 - T_4 - T_2) \quad (3-8)$$

This formula represents the generated power by the joule cycle. For the thermal efficiency calculation, the generated power is divided by the heat input into the system. [22]

$$\eta_{th} = \frac{\Delta\dot{W}_{ls}}{\dot{Q}_{12}} \quad (3-9)$$

$$\eta_{th} = \frac{\dot{m} \cdot c_p \cdot (T_3 + T_1 - T_4 - T_2)}{\dot{m} \cdot c_p \cdot (T_3 - T_2)} \quad (3-10)$$

$$\eta_{th} = \frac{(T_3 - T_2) + (T_1 - T_4)}{(T_3 - T_2)} \quad (3-11)$$

$$\eta_{th} = \frac{(T_3 - T_2)}{(T_3 - T_2)} + \frac{(T_1 - T_4)}{(T_3 - T_2)} = 1 + \frac{T_1 - T_4}{T_3 - T_2} \quad (3-12)$$

The joule cycle assumes an isobaric heat supply and heat dissipation. Therefore, there are only two different pressure levels p_1 and p_2 . This makes it possible to simplify the equation for thermal efficiency even more. The reason for this is the formula for the isentropic compression (or expansion). [17, 19] In the following formula γ is the isentropic exponent.

$$\frac{T_2}{T_1} = \left(\frac{p_1}{p_2}\right)^{\frac{\gamma-1}{\gamma}} = \frac{T_4}{T_3} \quad (3-13)$$

$$T_4 = T_3 \cdot \frac{T_2}{T_1} \quad (3-14)$$

This relation can be used to simplify the equation for cycle efficiency. [17, 19]

$$\eta_{th} = 1 + \frac{T_1 - T_4}{T_3 - T_2} = 1 + \frac{T_1 - T_3 \cdot \frac{T_2}{T_1}}{T_3 - T_2} = 1 + \left(\frac{T_1}{T_2}\right) \cdot \frac{T_3 - T_2}{T_3 - T_2} \quad (3-15)$$

$$\eta_{th} = 1 - \left(\frac{T_1}{T_2}\right) \cdot \frac{T_3 - T_2}{T_3 - T_2} \quad (3-16)$$

$$\eta_{th} = 1 - \left(\frac{T_1}{T_2}\right) = 1 - \left(\frac{p_2}{p_1}\right)^{\frac{(\gamma-1)}{\gamma}} \quad (3-17)$$

$$\eta_{th} = 1 - \left(\frac{p_2}{p_1}\right)^{\frac{(\gamma-1)}{\gamma}} \quad (3-18)$$

This formula states that the cycle efficiency of the ideal joule process is only dependent on the pressure levels p_1 and p_2 . In practical terms, this means that the difference between the upper and lower pressure limits defines the thermal efficiency of the cycle. Therefore the firing temperature has no impact on the thermal efficiency. [20] The firing temperature is essential for the thermal limitations of the turbine inlet. Therefore it limits the heat intake for a given pressure level. This limits the power the turbine can generate. [22]

4. Gas turbine parameters

Since there are different types of gas turbines, like radial and axial gas turbines, it is necessary to find a way to describe the fundamental behavior of these turbines. One example of an axial gas turbine is the SGT-800 (57 MW). Even within the axial gas turbines, the models can vary by the number of compressor and turbine stages [24]. In addition, they also vary in the firing temperature and the power generation. With all these parameters in mind, it is clear that it is nearly impossible to find basic behavioral patterns within the gas turbines based on dimensional parameters. This is because there are hundreds of turbines with different dimensions. It is important to note that the used temperatures and pressures are the stagnation temperatures and stagnations pressures if not mentioned otherwise.

Therefore non-dimensional parameters are used. These parameters aim to make operating points between different gas turbines comparable. They are used for plotting compressor and turbine maps. These diagrams illustrate the operating points of these components. For the determination of these non-dimensional parameters, dimensional analysis is used. [24]

For a further understanding, the process of dimensional analysis is explained in the following Chapter 4.1. Chapter 4.2 uses dimensional analysis for deriving important gas turbine performance parameters. These parameters are applied in the compressor and turbine maps. These diagrams are shown in Chapter 4.3.

4.1 Basics of dimensional analysis

Dimensional analysis makes it possible to rewrite a function where all parameters are dimensionless. If there is a function f with n input parameter and k different units, it is possible to create a function g with $n-k$ nondimensional input parameters. This is also called the Buckingham π -Theorem. [25, 26]

$$f(x_1, x_2, x_3, \dots, x_n) = 0 \quad (4-1)$$

This function f is formulated in a way where it is equal to zero. This is a valid assumption because every function can be rewritten in a way where its result is zero. This function has n parameters starting from x_1 and ending with x_n . All these parameters can have dimensions. In total, all these parameters have k different units. According to the Buckingham π -Theorem, it is possible to rewrite this function into a new one that only depends on dimensionless parameters. This new function is then called g . Since there are n parameters with k units, the new dimensionless function should have $n-k$ parameters. [25]

$$g(\pi_1, \pi_2, \pi_3, \dots, \pi_{n-k}) = 0 \quad (4-2)$$

It is demonstrated with the formula for the potential energy to show how it works. In this formula E_{pot} is the potential energy, ρ is the density, V is the volume, g is the gravitational acceleration and h is the height.

$$E_{pot} = \rho \cdot V \cdot g \cdot h \quad (4-3)$$

Since this formula is not equal to zero, it gets rewritten. After rewriting this formula, it is possible to see that there are five different parameters.

$$E_{pot} - \rho \cdot V \cdot g \cdot h = 0 \quad (4-4)$$

$$f(E_{pot}, \rho, V, g, h) = 0 \quad (4-5)$$

This calculation aims to create a function with only dimensionless input parameters. Therefore, it is necessary to know the dimension of each parameter. For this example, the input parameters and their units are shown in the following table.

Table 1: Used variables with their units

$\rho = \left[\frac{kg}{m^3} \right]$	$V = [m^3]$	$g = \left[\frac{m}{s^2} \right]$	$h = [m]$	$E_{pot} = \left[\frac{kg \cdot m^2}{s^2} \right]$
--	-------------	------------------------------------	-----------	---

These five parameters have three different units (kg, m, s). This means it is possible to rewrite this function with two dimensionless input parameters (5-3=2). Therefore these two non-dimensional parameters will be calculated. The potential energy, the density, and the volume are defined as repeater variables. The number of repeater variables is equal to the number of units [27]. This means that only the exponents for these three values get calculated and the exponent for the non-repeater variable is considered one. These exponents are calculated for every π -term. Each π -term consists of the repeater parameters and one other parameter.

$$\Pi_1 = E_{pot}^{e_1} \cdot \rho^{e_2} \cdot V^{e_3} \cdot g \quad (4-6)$$

$$\Pi_1 = \left(kg \cdot \frac{m^2}{s^2} \right)^{e_1} \cdot \left(\frac{kg}{m^3} \right)^{e_2} \cdot (m^3)^{e_3} \cdot \left(\frac{m}{s^2} \right) \quad (4-7)$$

Since the π -term is dimensionless, all the units have to erase themselves. Therefore, it is possible to formulate an equation for each unit. [25] In this equation, the exponent of a unit for a given input parameter is multiplied by the defined exponent e_1 , e_2 , or e_3 . This results in

three different equations for three variables. Therefore it is possible to calculate each of these three exponents.

$$kg: \quad 1 \cdot e_1 + 1 \cdot e_2 = 0 \quad (4-8)$$

$$e_1 = -e_2$$

$$s: \quad -2 \cdot e_1 - 2 = 0 \quad (4-9)$$

$$e_1 = -1$$

$$m: \quad 2 \cdot e_1 - 3 \cdot e_2 + 3 \cdot e_3 + 1 = 0 \quad (4-10)$$

$$2 \cdot (-1) - 3 \cdot (1) + 3 \cdot e_3 + 1 = 0$$

$$-4 + 3 \cdot e_3 = 0$$

$$e_3 = \frac{4}{3}$$

At this point, all given exponents are known. Therefore they can be inserted to calculate the first π -term.

$$\Pi_1 = E_{pot}^{e_1} \cdot \rho^{e_2} \cdot V^{e_3} \cdot g \quad (4-11)$$

$$\Pi_1 = \frac{\rho \cdot V^{\frac{4}{3}} \cdot g}{E_{pot}}$$

The second π -term gets calculated the same way the first one did. The only difference is that height instead of gravity is used. The repeater variables stay the same as in the first π -term.

$$\Pi_2 = E_{pot}^{e_1} \cdot \rho^{e_2} \cdot V^{e_3} \cdot h \quad (4-12)$$

$$\Pi_2 = \left(kg \cdot \frac{m^2}{s^2} \right)^{e_1} \cdot \left(\frac{kg}{m^3} \right)^{e_2} \cdot (m^3)^{e_3} \cdot m$$

$$kg: \quad 1 \cdot e_1 + 1 \cdot e_2 = 0 \quad (4-13)$$

$$e_1 = -e_2$$

$$s: \quad -2 \cdot e_1 = 0 \quad (4-14)$$

$$e_1 = 0$$

$$m: \quad 2 \cdot e_1 - 3 \cdot e_2 + 3 \cdot e_3 + 1 = 0 \quad (4-15)$$

$$2 \cdot (0) - 3 \cdot (0) + 3 \cdot e_3 + 1 = 0$$

$$e_3 = -\frac{1}{3}$$

$$\Pi_2 = E_{pot}^{e_1} \cdot \rho^{e_2} \cdot V^{e_3} \cdot h \quad (4-16)$$

$$\Pi_2 = E_{pot}^0 \cdot \rho^0 \cdot V^{-\frac{1}{3}} \cdot h$$

$$\Pi_2 = \frac{h}{V^{\frac{1}{3}}}$$

With both dimensionless input parameters calculated, the function g can be formulated as follows.

$$g(\Pi_1, \Pi_2) = 0 \quad (4-17)$$

$$g\left(\frac{\rho \cdot V^{\frac{4}{3}} \cdot g}{E_{pot}}, V^{\frac{1}{3}} \cdot h\right) = 0$$

The reason why this method is important for the modeling of gas turbines is that some of the most critical performance indicators are derived from this method. The advantage of these non-dimensional indicators is that they are practical for comparing performance characteristics for different machines [24]. Indicators like the Mach number, the normalized corrected mass flow, and the normalized corrected speed are derived with this method.

4.2 Important performance parameters of a gas turbine

This chapter explains some common non-dimensional performance parameters. These are the Mach number, the normalized corrected mass flow, and the normalized corrected speed .

4.2.1 The Mach number

One important non-dimensional parameter for describing the behavior of a gas turbine is the Mach number. The Mach number is defined as the ratio between the local flow speed u and the local speed of sound c [28].

$$Ma = \frac{u}{c} \quad (4-18)$$

The Mach number is an important parameter because the mass flow through a given diameter reaches the maximum mass flow with Mach one. If the Mach number is below one, the decrease in the fluid density is less compared to the increase in fluid speed. Therefore, the mass flow rises with an increased fluid speed. If the Mach number exceeds Mach one this is not true anymore. In this case, the density of the fluid decreases faster compared to the rise of the flow speed. This results in a decreasing mass flow despite increasing flow speed. This phenomenon is also called flow choking. [28] The Mach number is a dimensionless variable with a physical interpretation. Therefore, there are two ways to derive the Mach number. The first is to use the Buckingham π -theorem, and the second is to use the physical correlations.

Derivation of the Mach number with the Buckingham π -theorem

To use the Buckingham π -theorem for the derivation of the Mach number, it is necessary to define input parameters. The following derivation of the Mach number is inspired by the book “Fluid mechanics” by Çengel, Yunus A. and Cimbala, John M [27]. It is important to note that the following derivation of the Mach number uses similar parameters to the book but not the same ones. These input parameters are the speed of sound c , the mass flow \dot{m} , the specific volume v , and the flow area A .

Table 2: Variables needed for deriving the Mach number

$c = \left[\frac{m}{s} \right]$	$\dot{m} = \left[\frac{kg}{s} \right]$	$v = \left[\frac{m^3}{kg} \right]$	$A = [m^2]$
----------------------------------	---	-------------------------------------	-------------

With these parameters in mind, a non-dimensional flow speed is derived. All these combined parameters have three different units. These units are kg, s, and m. With four input parameters and three separate units, there is only one π -term. This π -term will be calculated using the following equation.

$$f(c, v, A, \dot{m}) = 0 \quad (4-19)$$

In this case, the mass flow, the diameter, and the characteristic density are used as repeater variables.

$$\Pi_1 = \dot{m}^{e_1} \cdot A^{e_2} \cdot v^{e_3} \cdot c \quad (4-20)$$

$$\Pi_1 = \left(\frac{kg}{s}\right)^{e_1} \cdot (m^2)^{e_2} \cdot \left(\frac{m^3}{kg}\right)^{e_3} \cdot \left(\frac{m}{s}\right)$$

This π -term can be calculated using the three following equations.

$$kg: \quad 1 \cdot e_1 - 1 \cdot e_3 = 0 \quad (4-21)$$

$$e_1 = e_3$$

$$m: \quad 2 \cdot e_2 + 3 \cdot e_3 + 1 = 0 \quad (4-22)$$

$$e_2 = -\frac{3}{2} \cdot e_3 - \frac{1}{2}$$

$$s: \quad -1 \cdot e_1 - 1 = 0 \quad (4-23)$$

$$e_1 = -1$$

$$e_3 = e_1 = -1 \quad (4-24)$$

$$e_2 = -\frac{3}{2} \cdot e_3 - \frac{1}{2} = -\frac{3}{2} \cdot (-1) - \frac{1}{2}$$

$$e_2 = 1$$

$$\Pi_1 = \dot{m}^{-1} \cdot A^1 \cdot v^{-1} \cdot c \quad (4-25)$$

$$\Pi_1 = \frac{A \cdot c}{\dot{m} \cdot v}$$

As defined earlier, the Mach number is the local flow speed divided by the local speed of sound.

$$\Pi_1 = \frac{A \cdot c}{\dot{m} \cdot v} = \frac{A \cdot c}{\dot{V}} = \frac{c}{u} = \frac{1}{Ma} \quad (4-26)$$

$$Ma = \frac{u}{c}$$

This is one way to derive the Mach number. Since these non-dimensional parameters are often helpful for comparing different turbomachines, there is no need for a physical derivation of these parameters. In the case of the Mach number, one will also be shown nevertheless.

Physical derivation of the Mach number

For calculating the Mach number, the speed of sound is needed. The speed of sound is the speed at which an infinitesimally pressure waves can travel through a given medium [27]. It is dependent on multiple parameters and can change though out the turbomachine [29]. Since the speed of sound is not constant, the literature often mentions the local speed of sound. The local speed of sound is the speed of sound at a given point within the turbomachine. For calculating the Mach number, the measured flow speed and the local speed of sound at the measurement point have to be used. For the derivation of the Mach number, the first step is to calculate the maximal speed of a pressure wave in a fluid. This speed is equal to the speed of sound. For this deviation, the continuity equation is used. In this equation, \dot{m} is the mass flow, ρ is the density, A is the flow area, and u is the flow speed if the fluid [30].

$$\dot{m} = \rho \cdot \dot{V} = \rho \cdot A \cdot u \quad (4-27)$$

This formula shows that for a given diameter and a constant mass flow, a change in velocity also creates a change in density if the mass flow and the diameter are considered constant.

$$\dot{m}_1 = \dot{m}_2 \quad (4-28)$$

$$\rho_1 \cdot A \cdot u_1 = \rho_2 \cdot A \cdot u_2 \quad (4-29)$$

$$\rho_1 \cdot u_1 = \rho_2 \cdot u_2 \quad (4-30)$$

This formula will be used as starting point to determine how fast a pressure wave travels through the fluid.

The derivation follows that of the book “Fundamentals of Compressible Fluid Mechanics” by Bar-Meir Genick [31]. In the following equation du represents the fluid's local flow speed. In the following formula, dp is the change in density, and c is the speed of the pressure wave. The assumption is that the pressure wave travels against the flow direction. Therefore its sign is negative.

$$\rho \cdot c = (\rho + d\rho) \cdot (c - du) \quad (4-31)$$

$$\rho \cdot c = \rho \cdot c + \rho \cdot du - c \cdot d\rho + d\rho du \quad (4-32)$$

The term $d\rho$ multiplied by du will be neglected. Therefore, it is set equal to zero. Therefore, this formula can be simplified to the following equation.

$$d\rho du = 0 \quad (4-33)$$

$$0 = \rho \cdot du - c \cdot d\rho \quad (4-34)$$

This formula represents the final form of the continuity equation.

$$c \cdot d\rho = \rho \cdot du \quad (4-35)$$

For the next step, the Bernoulli equation is used. In this equation, c represents the local speed of sound, u represents the fluid's local flow speed, and the variable p represents the pressure.

$$\frac{(c - du)^2 - c^2}{2} + \frac{dp}{\rho} = 0 \quad (4-36)$$

$$\frac{c^2 - 2 \cdot c \cdot du + (du)^2 - c^2}{2} + \frac{dp}{\rho} = 0 \quad (4-37)$$

The term $(du)^2$ is also considered neglectable and set equal to zero. This results in the following formula.

$$(du)^2 = 0 \quad (4-38)$$

$$-c \cdot du + \frac{dp}{\rho} = 0 \quad (4-39)$$

The two following formulas represent the formulas of the continuity equation and the Bernoulli equation. Both of these formulas are rewritten in a way that the differential of the flow speed is on the left side of the equation.

$$du = \frac{c}{\rho} \cdot d\rho \quad (4-40)$$

$$du = \frac{1}{\rho \cdot c} \cdot dp \quad (4-41)$$

These two equations are set equal in the next step.

$$\frac{c}{\rho} \cdot d\rho = \frac{1}{\rho \cdot c} \cdot dp \quad (4-42)$$

The formula is now able to calculate the local speed of sound. In literature, this equation is often represented by the second formulation.

$$c^2 \cdot d\rho = dp \quad (4-43)$$

$$c = \sqrt{\frac{dp}{d\rho}} \quad (4-44)$$

The equation (4-44) and the simplified version of the Bernoulli equation are rewritten in the next step so that the pressure differential is on the left side of the equation.

$$dp = \rho \cdot c \cdot du \quad (4-45)$$

$$dp = c^2 \cdot d\rho \quad (4-46)$$

These two equations are set equal in the next step.

$$\rho \cdot c \cdot du = c^2 \cdot d\rho \quad (4-47)$$

$$c = \rho \cdot \frac{du}{d\rho} \quad (4-48)$$

This relation of the local speed of sound is used for replacing the speed of sound in the formula of the Mach number.

$$Ma = \frac{u}{c} \quad (4-49)$$

$$Ma = \frac{u}{c} = u \cdot \frac{1}{\rho} \cdot \frac{d\rho}{du} \quad (4-50)$$

$$\frac{du}{u} \cdot Ma = \frac{d\rho}{\rho} \quad (4-51)$$

This formula shows that if the Mach number is below one, the density change in the fluid is smaller than the change in the velocity. In this case, the mass flow of the fluid would rise. If the Mach number is equal to one, the velocity change would be similar to the density change of the fluid. If the Mach number exceeds one, then the density of the fluid drops faster than the velocity rises. This would result in a decrease in the mass flow [28]. This is why the mass flow can not be increased above Mach one. This phenomenon is also called flow choking.

Therefore, flow choking is an essential aspect to be considered in the design process. A turbine often operates near Mach one. The Mach number can change if operating conditions change for a turbine or a compressor. Since the Mach number has no dimension, it is possible to describe and compare the characteristics of different turbines and compressors. One important aspect is that above a Mach number of 0.3, a fluid must be calculated as compressible [15]. Therefore, it is mainly impossible to assume an incompressible fluid for the simulation of gas turbines.

4.2.2 The normalized corrected mass flow

The normalized corrected mass flow is like the Mach number, also a non-dimensional parameter. It is often used for describing the mass flow through a turbine or a compressor [28]. The reason why the mass flow is not used instead is to make it more comparable. If this parameter was dimensional, it would not be comparable to other turbomachines. In addition to the normalized corrected mass flow, the corrected mass flow is also often mentioned in literature. The difference between these two is that the normalized corrected mass flow $NCFLW$ is a given corrected mass flow $CFLW_{in}$ divided by the reference one $CFLW_{Ref}$.

$$NCFLW = \frac{CFLW_{in}}{CFLW_{Ref}} \quad (4-52)$$

The corrected mass flow is derived with the Buckingham π -theorem. In literature, the corrected mass flow gets derived with a handful of other non-dimensional performance indicators. Therefore, more parameters are used in the literature. The following paragraph shows only the variables necessary for this derivation. The needed variables are the density ρ , the local speed of sound c , the diameter D , and the mass flow m . The following derivation of

the corrected flow from equation (4-53) till equation (4-66) is inspired by the book “Fundamentals of Turbomachines” by Erik Dick [23].

Table 3: Variables used for deviating the normalized corrected flow

$\rho = \left[\frac{kg}{m^3} \right]$	$c = \left[\frac{m}{s} \right]$	$D = [m]$	$\dot{m} = \frac{kg}{s}$
--	----------------------------------	-----------	--------------------------

Since there are only four parameters with three different units, this results in only one non-dimensional parameter. This parameter will be the corrected mass flow.

$$F(\rho, c, D, \dot{m}) = 0 \quad (4-53)$$

$$\Pi_1 = \rho^{e_1} \cdot c^{e_2} \cdot D^{e_3} \cdot \dot{m} \quad (4-54)$$

$$\Pi_1 = \left(\frac{kg}{m^3} \right)^{e_1} \cdot \left(\frac{m}{s} \right)^{e_2} \cdot m^{e_3} \cdot \left(\frac{kg}{s} \right) \quad (4-55)$$

$$kg: \quad 0 = e_1 + 1 \quad (4-56)$$

$$e_1 = -1$$

$$s: \quad 0 = -e_2 - 1 \quad (4-57)$$

$$e_2 = -1$$

$$m: \quad 0 = -3 \cdot e_1 + e_2 + e_3 \quad (4-58)$$

$$0 = -3 \cdot (-1) - 1 + e_3$$

$$e_3 = -2$$

$$\Pi_1 = \rho^{e_1} \cdot c^{e_2} \cdot D^{e_3} \cdot \dot{m} = \rho^{-1} \cdot c^{-1} \cdot D^{-2} \cdot \dot{m} \quad (4-59)$$

$$\Pi_1 = \frac{\dot{m}}{\rho \cdot c \cdot D^2} \quad (4-60)$$

This non-dimensional parameter represents the non-dimensional mass flow. It looks different from the literature's formulations because it must be modified. Therefore, the ideal gas equation is used.

$$\rho = \frac{p}{R_s \cdot T} \quad (4-61)$$

Now this formula is used to rewrite the density in the non-dimensional parameter.

$$CFLW = \frac{\dot{m} \cdot R_s \cdot T}{p \cdot c \cdot D^2} \quad (4-62)$$

In the next step, the formula for the local speed of sound is used.

$$c = \sqrt{\gamma \cdot R_s \cdot T} \quad (4-63)$$

This relation is used to replace the local speed of sound in the formula for the corrected mass flow.

$$CFLW = \frac{\dot{m} \cdot R_s \cdot T}{p \cdot \sqrt{\gamma \cdot R_s \cdot T} \cdot D^2} \quad (4-64)$$

$$CFLW = \frac{\dot{m} \cdot \sqrt{R_s \cdot T}}{p \cdot \sqrt{\gamma} \cdot D^2} \quad (4-65)$$

$$CFLW = \frac{\dot{m} \cdot \sqrt{T}}{p} \cdot \frac{\sqrt{R_s}}{\sqrt{\gamma} \cdot D^2} \quad (4-66)$$

This non-dimensional parameter is split into two parts. The first part includes the mass flow, the temperature, and the pressure. This part of the formula changes for different operating conditions. For a given turbine and working fluid, it is usual to drop the gas constant, the isentropic exponent, and the diameter [28]. This reduces the formula of the corrected mass flow to the following expression.

$$CFLW = \frac{\dot{m} \cdot \sqrt{T}}{p} \quad (4-67)$$

It is important to note that the reduced formula for the corrected mass flow is not dimensionless anymore. In addition to this, the corrected mass flow is not normalized. Therefore, it is common in the literature to normalize this corrected mass flow. For normalization, a reference point is needed. This is often the point with the highest corrected mass flow, but this is not mandatory. If another reference point is used, the normalized

corrected mass flow may exceed the value of one. The following expression represents the reference corrected mass flow.

$$CFLW_{ref} = \frac{\dot{m}_{ref} \cdot \sqrt{T_{ref}}}{p_{ref}} \quad (4-68)$$

Every operating point of the turbine with a corrected mass flow gets now divided by this reference point. [28]

$$CFLW_{in} = \frac{\dot{m}_{in} \cdot \sqrt{T_{in}}}{p_{in}} \quad (4-69)$$

$$NCFLW = \frac{\dot{m}_{in}}{\dot{m}_{ref}} \cdot \frac{p_{ref}}{p_{in}} \cdot \sqrt{\frac{T_{in}}{T_{ref}}} \quad (4-70)$$

After this normalization, the normalized corrected mass flow is now non-dimensional again. Using a reference point also indicates why dropping the three parameters from before is possible. This is because the turbine diameter stays the same at every operating point. Therefore, this variable would always be one after the normalization. The same is also true for the gas constant. The isentropic exponent is considered constant, because the gas is considered perfect [28]. With the assumption that the turbine operates only in a temperature range where the isentropic exponent does not change very much, it can be neglected.

Even though the formula above represents the normalized corrected mass flow, it looks slightly different in the literature. The reason for this is that the pressure ratio and the temperature ratio are often represented as follows.

$$\theta = \frac{T_{in}}{T_{ref}} \quad (4-71)$$

$$\delta = \frac{p_{in}}{p_{ref}} \quad (4-72)$$

$$NCFLW = \frac{\dot{m}_{in}}{\dot{m}_{ref}} \cdot \frac{\sqrt{\theta}}{\delta} \quad (4-73)$$

If the normalized corrected mass flow is assumed as one, it is possible to calculate the reference mass flow. [24]

$$NCFLW = 1 = \frac{\dot{m}_{in}}{\dot{m}_{ref}} \cdot \frac{\sqrt{\theta}}{\delta} \quad (4-74)$$

$$\dot{m}_{ref} = \dot{m}_{in} \cdot \frac{\sqrt{\theta}}{\delta} \quad (4-75)$$

This so calculated mass flow represents an equivalent mass flow for reference conditions. [24]

4.2.3 The normalized corrected speed

The normalized corrected speed is based on the corrected speed. This corrected speed can be derived from the Buckingham π -theorem. To achieve this, only four parameters are needed. These four parameters are the density ρ , the local speed of sound c , the diameter D , and the rotational speed Ω . The following derivation of the corrected flow from equation (4-76) till equation (4-84) is inspired by the book "Fundamentals of Turbomachines" by Erik Dick [23].

Table 4: The used variables with their units

$\rho = \left[\frac{kg}{m^3} \right]$	$c = \left[\frac{m}{s} \right]$	$D = [m]$	$\Omega = \left[\frac{1}{s} \right]$
--	----------------------------------	-----------	---------------------------------------

In this case, these four parameters are also set up like in the derivation before.

$$F(\rho, c, D, \Omega) = 0 \quad (4-76)$$

$$\Pi_1 = \rho^{e_1} \cdot c^{e_2} \cdot D^{e_3} \cdot \Omega \quad (4-77)$$

$$\Pi_1 = \left(\frac{kg}{m^3} \right)^{e_1} \cdot \left(\frac{m}{s} \right)^{e_2} \cdot m^{e_3} \cdot \left(\frac{1}{s} \right)$$

$$kg: \quad 0 = e_1 \quad (4-78)$$

$$s: \quad 0 = -e_2 - 1 \quad (4-79)$$

$$e_2 = -1 \quad (4-80)$$

$$m: \quad 0 = -3 \cdot e_1 + e_2 + e_3 \quad (4-81)$$

$$0 = -3 \cdot (0) - 1 + e_3$$

$$e_3 = 1$$

$$\Pi_1 = \rho_{01}^{e_1} \cdot a_{01}^{e_2} \cdot D^{e_3} \cdot \Omega = \rho_{01}^0 \cdot a_{01}^{-1} \cdot D^1 \cdot \Omega \quad (4-82)$$

$$\Pi_1 = \frac{\Omega \cdot D}{c}$$

This term π_1 represents the corrected speed. At this point, it looks a bit different from the literature. This is because the turbine's diameter and the sound's local speed are present in this formula. As shown earlier, the local speed of sound has the following formula.

$$c = \sqrt{\gamma \cdot R_s \cdot T} \quad (4-83)$$

Therefore, this formula can replace the local speed of sound. This creates the following expression.

$$CS = \frac{\Omega \cdot D}{\sqrt{\gamma \cdot R_s \cdot T}} \quad (4-84)$$

$$CS = \frac{\Omega}{\sqrt{T}} \cdot \frac{D}{\sqrt{\gamma \cdot R_s}}$$

This formula for the corrected speed is split into two parts. The first part of this formula changes with the operating point, and the second part nearly stays constant. In the literature, dropping the diameter, the isentropic exponent, and the gas constant is typical [28]. This results in the following expression.

$$CS = \frac{\Omega}{\sqrt{T}} \quad (4-85)$$

Since the three parameters got dropped, this expression is not dimensionless anymore. To make this parameter non-dimensional again, it is divided by a reference point. [24]

$$CS_{ref} = \frac{\Omega_{ref}}{\sqrt{T_{ref}}} \quad (4-86)$$

$$CS_{in} = \frac{\Omega_{in}}{\sqrt{T_{in}}} \quad (4-87)$$

$$NCS = \frac{CS_{in}}{CS_{ref}} = \frac{\Omega_{in}}{\Omega_{ref}} \cdot \sqrt{\frac{T_{ref}}{T_{in}}} \quad (4-88)$$

The normalized corrected speed can exceed values above one if the corrected speed used as reference is not the highest for a given operating point set. Since a reference point normalized the normalized corrected speed, the gas constant and the diameter of the turbine would have been canceled out. Therefore, it is easy to see why it is possible to drop these two constants. This is only a valid approximation for the isentropic exponent if the temperature varies not much for different operating points.

If the normalized corrected speed is assumed to be one, it is possible to calculate a turbine's or compressor's reference rotational speed for a given operating point. This makes it possible to compare the rotational speed of a given operating point with the rotational speed by reference conditions. [24]

$$NCS = 1 = \frac{\Omega_{in}}{\Omega_{ref}} \cdot \sqrt{\frac{T_{ref}}{T_{in}}} \quad (4-89)$$

$$\Omega_{ref} = \frac{\Omega_{in}}{\sqrt{\frac{T_{in}}{T_{ref}}}} \quad (4-90)$$

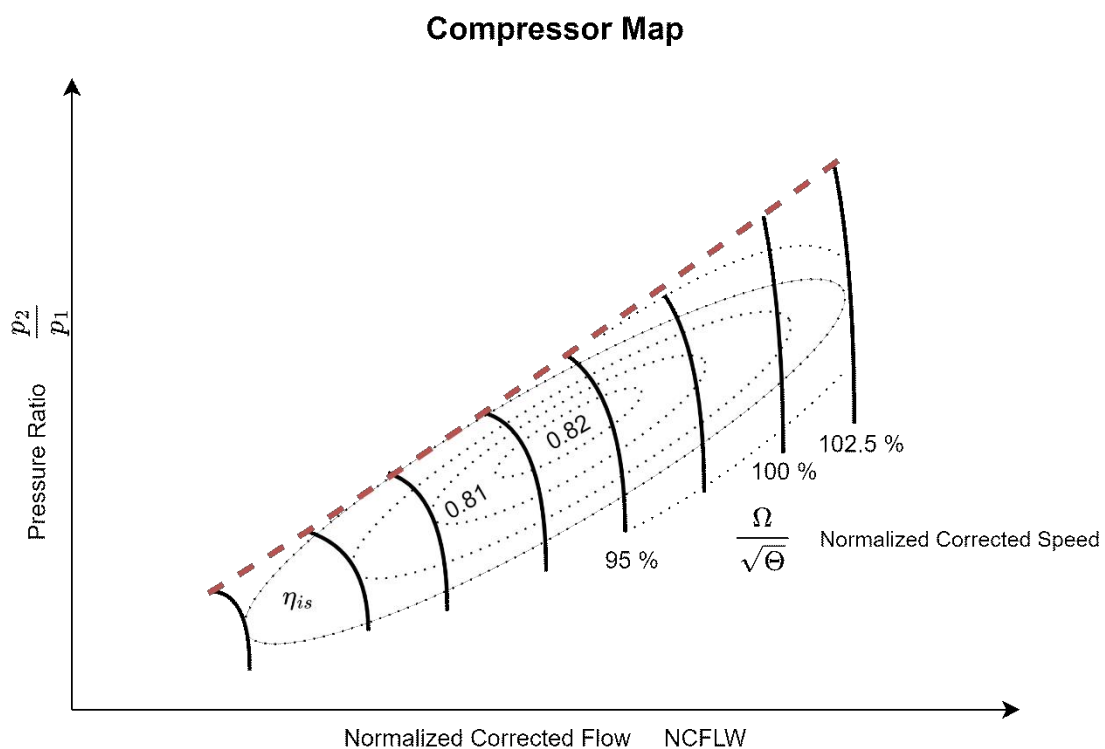
This formulation of the normalized corrected speed is commonly used in literature. The result of this expression is the rotational speed the turbine would have by reference conditions.

4.3 Performance maps

Gas turbine performance maps are used for describing the behavior of the compressor or turbine for different operating points. These maps only use non-dimensional parameters. Even though the maps change for different compressors or turbines, the basic characteristics stay similar.

4.3.1 Compressor map

The normalized corrected mass flow and the normalized corrected speed are used to create the compressor map. This map also uses the pressure ratio of the compressor. The compressor map is a way to characterize the behavior of a compressor. The compressor map plots the normalized corrected mass flow against the pressure ratio. In this map, there is also the normalized corrected speed and the isentropic efficiency represented. [28]



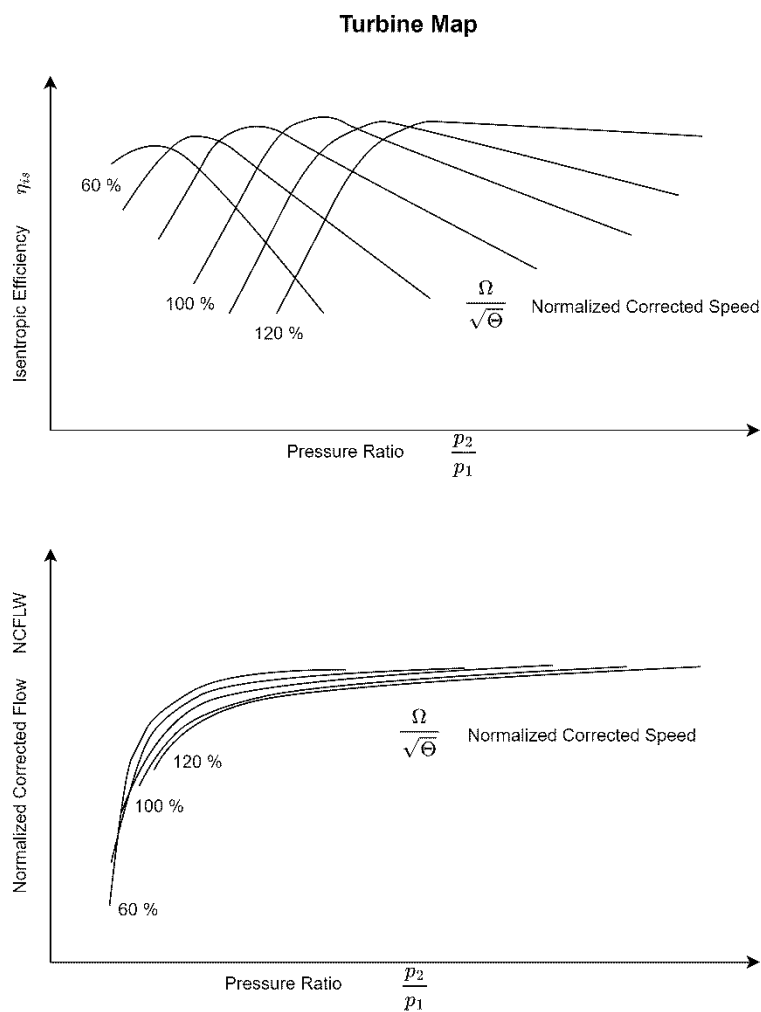
4-1: Example of a compressor map inspired by [28]

A compressor map can be created through extensive testing and measuring or computer simulation [32]. This map makes it possible to predict the behavior of a compressor for different conditions. One critical line in this map is the surge line. If the pressure level rises for a given normalized corrected mass flow above a defined limit, the compressor will surge. This happens when the speed of the fluid exceeds Mach one. After this point, the density of the fluid starts dropping, and the mass flow cannot be increased. If a work line for a compressor

is known, it is possible to predict the isentropic efficiency and the corrected speed. It is possible to check if the compressor will not exceed a specific pressure limit and stall. [28] Since the compressor map is created with non-dimensional indicators, the compressor maps of different compressors look similar, which makes them easy to read and use.

4.3.2 Turbine map

The characteristic operation behavior of the turbine gets plotted into a so-called turbine map. Since all these parameters are normalized and non-dimensional it is possible to compare this turbine map with others. This turbine maps are often based on experimental data [33].



4-2: Example of a turbine map inspired by [28]

These plots both have the pressure ratio on the x-axis. In the first plot the isentropic efficiency is represented on the y-axis. In the second plot the y-axis shows the normalized corrected mass flow. These four parameters are important for characterizing the behavior of a turbine. [28]

5. Creating a simulation model

This chapter starts by explaining the principles of the correction curve model. After this, the physical simulation model will be described. This begins with the basic idea of the simulation model (Chapter 5.2) and ends by implementing the gas turbine model in Epsilon Professional (Chapter 5.2.1 - 5.2.9). The used regressions in the physical simulation model will then be fitted by the Reference Run (Chapter 5.4). The Validation Run will then validate this fitted model (Chapter 5.5). The last step is to change the fuel from methane to hydrogen in the Hydrogen Run (Chapter 5.6).

5.1 The Correction Curve Model

To understand why the correction curve model can not be used for predicting a hydrogen-powered gas turbine, it is essential to know how a correction curve model works. First, the correction curve model does not represent a physical simulation [34]. Instead, it uses multiple functions to predict specific parameters like the air mass flow, fuel mass flow, temperature of the flue gas, and the power generated. These functions are all based on ambient temperature, pressure, and humidity. A function applies a correction factor to the prediction for each parameter change. Therefore, the prediction of this correction curve model is not the result of a physical simulation. Instead, it results from multiple functions applying multiple correction factors to a default prediction.

The function for applying a specific correction factor can even change depending on the surroundings. Parameters like ambient humidity use a different function for calculating a correction factor based on the ambient temperature. The advantage of this approach is that the correction curve model can deliver the same results as an actual gas turbine without complex modeling [34]. The only thing needed is multiple operating points for the gas turbine to calculate these correction functions based on the ambient conditions. Since these functions only use the ambient conditions as parameters for their predictions, they are only valid for the intended fuel. In the example of the SGT-800 (57 MW), these functions are only valid for natural gas. As a result, they would not take the fuel change into account. Therefore, the correction curve model of the SGT-800 (57 MW) gas turbine cannot predict the behavior caused by a fuel change to hydrogen.

5.2 Reverse engineering the physical model

This thesis aims to create a physical model of the SGT-800 (57 MW) gas turbine. This model is then used for predicting the turbines behavior when it is powered with hydrogen. Therefore, the first step is to create a physical model of the SGT-800 (57 MW) gas turbine. This model is divided into four main parts.

1. Compressor
2. Combustion system
3. Turbine
4. Generator

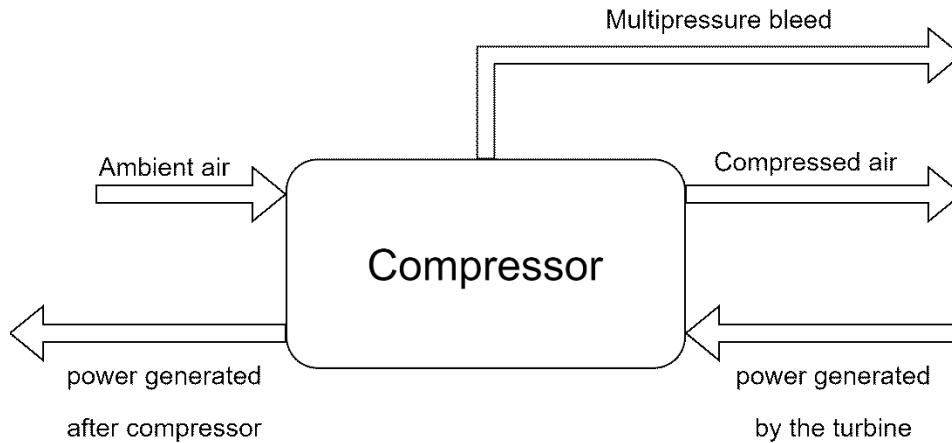
Each of these components is modeled in Epsilon Professional. The combination of these components represents the gas turbine model. These components will use regressions to predict specific parameters like the air mass flow or the exhaust temperature. Without these regressions, the physical model will not be able to work independently. Since regressions need data to fit, the physical model must take these values from the correction curve model. This is done for multiple scenarios. This run aims to generate data unavailable in the correction curve model for fitting the regressions. This run is referred to as the Reference Run.

The physical model can work independently with this data and the so-fitted regression. At this point, the model must be validated. Therefore, multiple scenarios are calculated for the physical model and the correction curve model. This is also referred to as the Validation Run. At this point, there is no data transfer between these two models. It is considered reliable if the physical model creates a close enough result compared to the correction curve model.

This validated physical model is then used for predicting the gas turbine's behavior if the fuel changes from methane to hydrogen. The same scenarios are calculated in this so-called Hydrogen Run as in the Validation Run. The only difference between these two datasets is the fuel used by the gas turbine. Therefore, this dataset will then be interpreted for similarities and differences.

5.2.1 Modeling concept of the compressor

The purpose of the compressor is to raise the pressure level of the air mass flow at its inlet [13]. This compressed air flows then to the combustion chamber. The physical model of the compressor should be able to calculate the air mass flow, and the power needed to reach a given pressure level. The schematic of this component can be seen in the following diagram.



5-1: Schematic function of the compressor model

The compressor will not be modeled with multiple bleed flows. Therefore, the mass flow can be described using equation (5-1). In the formula \dot{m}_{In} is the air mass flow in the compressor, \dot{m}_{Out} is the air mass flow out of the compressor and \dot{m}_B are the summed up bleed flows to the turbine.

$$\dot{m}_{In} = \dot{m}_{Out} + \dot{m}_B \quad (5-1)$$

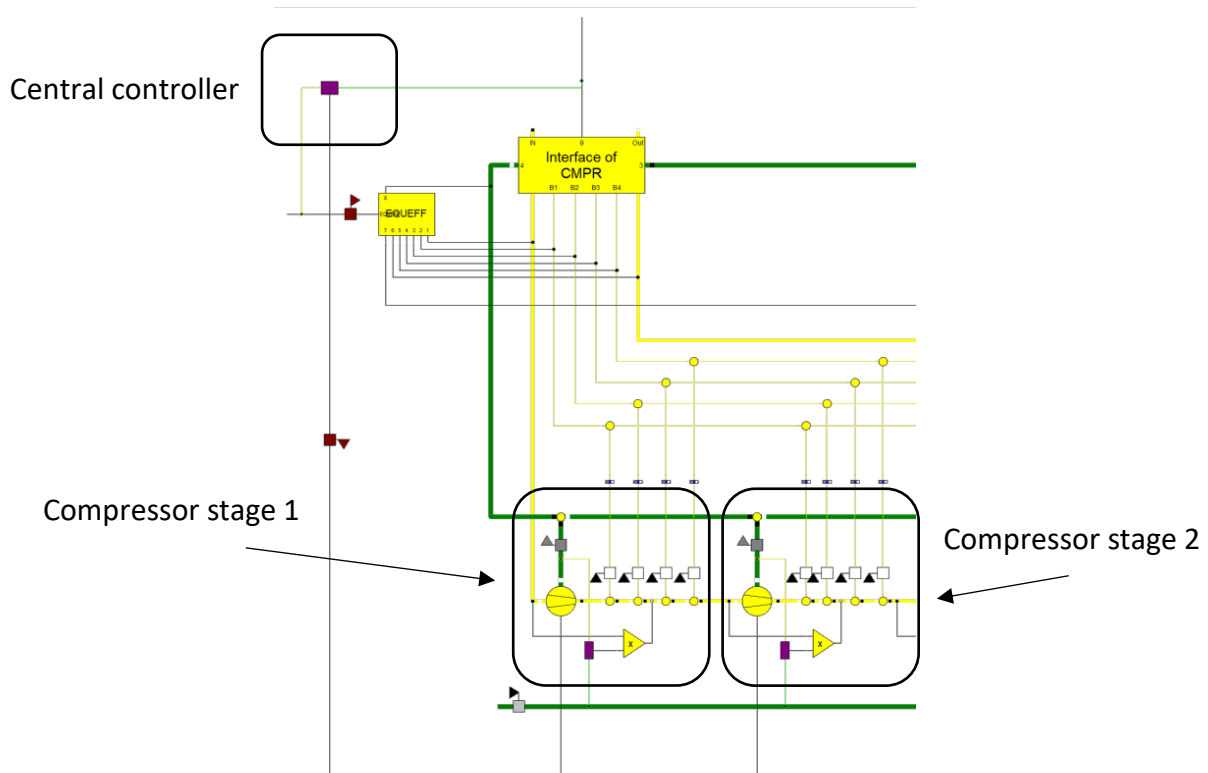
The compressor and the turbine sit on the same shaft. Therefore, they have the same rotational speed. This rotational speed is constant with 6608 1/min [35]. The compressor only uses ambient conditions to predict the air mass flow at its inlet. It is important to note that this compressor has multiple bleed flows with different pressure levels. Therefore, the power consumption calculated by the compressor model must take all these flows and their pressure level into account. This power P_{Comb} is then subtracted from the power generated by the turbine P_{Turb} . The resulting power P_{Gen} can be used for power generation [24].

$$P_{Gen} = P_{Turb} - P_{Comb} \quad (5-2)$$

It is important to note that the compressor model will not be able to predict an exit pressure level. Therefore, it has to be defined externally.

5.2.2 Modeling the compressor in Epsilon Professional

The compressor of the gas turbine SGT-800 (57 MW) consists of 15 stages [36]. Each of these 15 stages is modeled as a compressor itself. Therefore, each stage uses the compressor component (Comp 24) in Epsilon Professional. The mechanical energy used by each stage is considered constant [24]. In the modeling of the compressor, there are multiple controllers (Comp 12) used. Since the pressure level of the compressor exit is set externally, one central controller raises the power consumption for each stage until the compressor meets the requested pressure level. In addition to this, there is a controller for each stage. This stage controller aims to raise the power consumption for its stage to meet the defined power consumption set by the central controller. The reason for these stage controllers is to ensure that each stage uses the same amount of power. It is also important to note that the pressure rise in each stage is therefore not constant. A section of the implemented compressor is shown in the following figure.

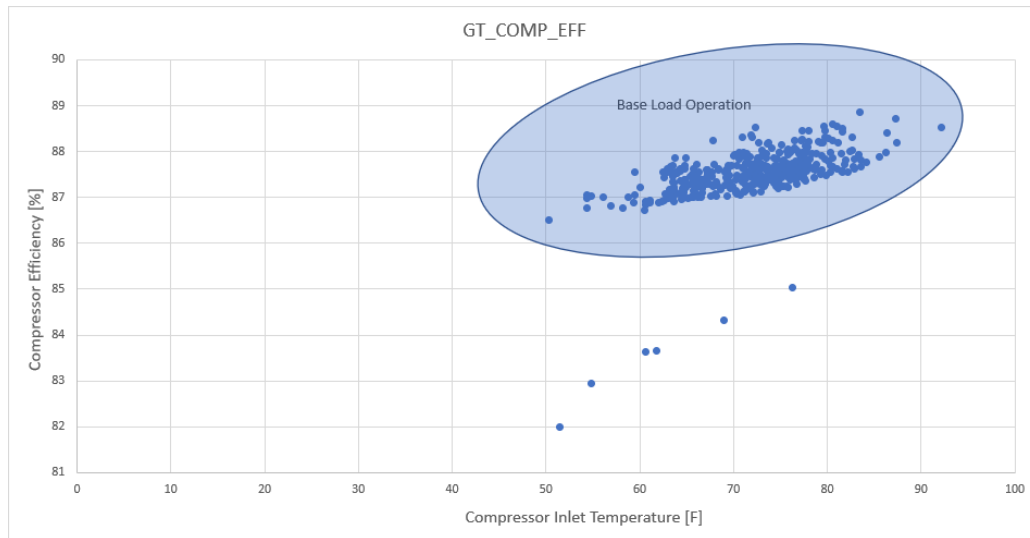


5-2: Part of the modeled compressor

Another important aspect of this compressor model is that the pressure ratio is not constant for different environmental conditions. Therefore, the pressure ratio changes with the surrounding pressure, temperature, and humidity.

One design aspect of the compressor is that the isentropic efficiency is fixed to 85 percent.

This design decision is based on the communication with two Experts from ENEXSA GmbH. They used the following example figure (5-3) for illustration.



5-3: Compressor Efficiency for Base Load Operation

“Typical compressor efficiencies as a function of ambient temperature taken from an online performance monitoring system (Pechtl, Pölzl, ENEXA GmbH, Private Communication Undisclosed client). Full load efficiencies vary in a relatively narrow band.”

Based on this communication, the isentropic efficiency of the compressor is set constant.

The main compressor is modeled with multiple stages, each of which has optional bleed flows. This makes the calculation of the isentropic efficiency more complex. In this case, the isentropic efficiency is calculated based on each inlet and outlet flow of the compressor. The compressor has only one inlet stream. Therefore, its enthalpy and entropy can be considered the starting point of the compression. For each outgoing stream, the pressure is measured. With the pressure and the entropy of the inlet stream, it is possible to calculate the isentropic enthalpy of the outlet stream for the measured pressure. The difference between the isentropic outlet enthalpy and the enthalpy of the inlet stream multiplied by the mass flow of the outlet stream is the minimum power needed for the compression. This calculation is done for each of the outlet streams and added up. The result is the isentropic power needed for the compression to the multiple pressure levels of the outlet streams. The formula (5-3) calculates this isentropic power. In this formula, W_{is} is the isentropic power. H_2 is the specific enthalpy of the gas at the compressor outlet. H_1 represents the enthalpy of the fluid at the inlet of the compressor. The variable m_2 is the mass flow at the compressor exit. The specific enthalpy H_{Bi} and the mass flow m_{Bi} represent the multiple bleed flows.

$$\dot{W}_{is} = (H_2 - H_1) \cdot \dot{m}_2 + \sum_{i=1}^n (H_{Bi} - H_1) \cdot \dot{m}_{Bi} \quad (5-3)$$

This isentropic power can then be divided by the consumed power of the compressor W_{real} . The result is the formula for the isentropic efficiency of the compressor [37].

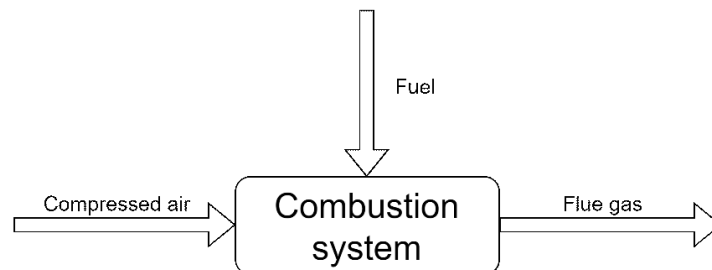
$$\eta_{is} = \frac{\dot{W}_{is}}{\dot{W}_{real}} \quad (5-4)$$

In the model, the isentropic efficiency is constantly calculated. This is because one controller changes the efficiency of all stages to meet the defined compressor efficiency of 85%. At this point, the compressor model can hold a constant isentropic efficiency of 85% for different ambient conditions and multiple bleed flows. The model can also calculate the power consumption for a given pressure level. At this stage, the physical model of the compressor can simulate the compression for a given inlet stream and multiple bleed flows.

As explained before, the compressor model should also be able to predict the air mass flow at its inlet. Therefore this model needs predefined ambient conditions. The air mass flow changes for different ambient conditions therefore, a multivariant polynomial regression is used. This regression aims to predict the air mass flow in the compressor based on the surrounding conditions. The exact creation of this regression is explained later.

5.2.3 Modeling concept of the combustion system

The combustion system is one of the critical aspects of the physical model. It inherits the fuel control system. The combustion system aims to define the fuel mass flow. The schematic of the combustion system is shown in the following figure.



5-4: Schematic function of the combustion system

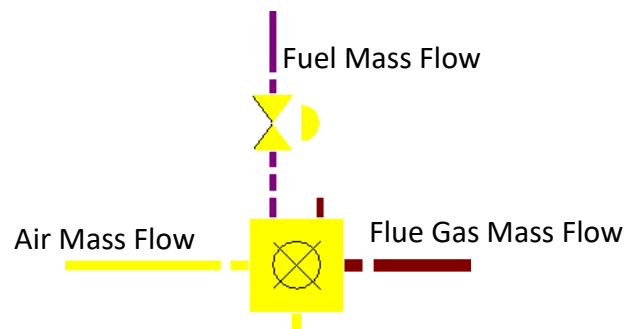
Since the mass flow of compressed air \dot{m}_A is defined by the compressor and the fuel mass flow \dot{m}_F is defined by the combustion system, it is possible to calculate the mass flow of the flue gas \dot{m}_{FG} with the following formula.

$$\dot{m}_{FG} = \dot{m}_A + \dot{m}_F \quad (5-5)$$

The combustion system also calculates the flue gas's composition and firing temperature. As indicated in the joule cycle, the combustion is performed isobaric. This is the reason why the exit pressure level of the compressor is equal to the inlet pressure level of the turbine.

5.2.4 Modeling the combustion system in Epsilon Professional

In Epsilon Professional, the modeled combustion system mainly consists of the combustion chamber component (Comp 22). This component takes the compressed air mass flow, and the fuel mass flow as inputs and calculates the resulting flue gas flow. This component's calculation results include fuel gas composition and firing temperature. It is implemented in Epsilon Professional as follows.



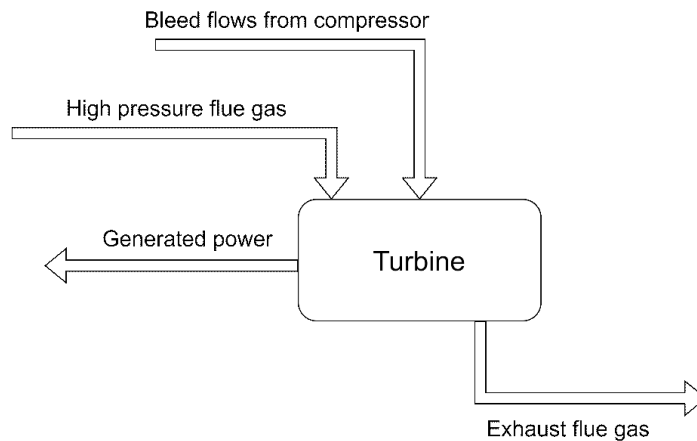
5-5: Combustion system in Epsilon Professional

The fuel pressure is 32 bar, and the temperature is 15 °C [12]. These values are based on the correction curve model and are constant for all calculations. To predict the fuel mass flow a multivariant polynomial regression will be used. This regression will predict the turbine exhaust temperature. The controller will then regulate the fuel to meet this temperature.

5.2.5 Modeling concept of the turbine

The primary purpose of a turbine is to expand the high temperature and pressure flue gas for power generation. Therefore the turbine model must be able to calculate the power generated by the expansion of the flue gas. In addition, it also has to calculate the inlet pressure level and the exhaust temperature of the flue gas. As mentioned before, the inlet pressure level of the turbine is equal to the exit pressure level of the compressor. Therefore this turbine model is responsible for calculating the exit pressure level of the compressor too.

The turbine must also take bleed flows from the compressor into account. The schematic of the turbine model looks like this.



5-6: Schematic function of a turbine

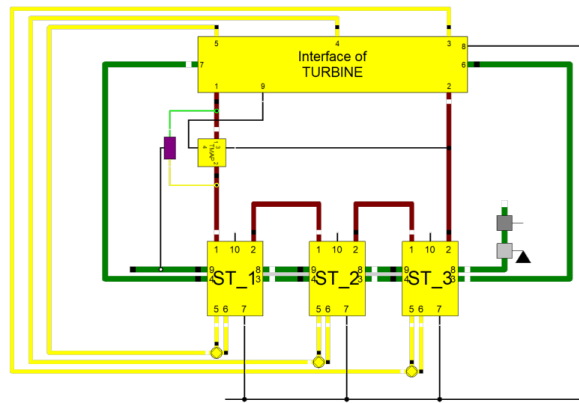
The high-pressure flue gas \dot{m}_{FG} flows directly from the combustion chamber in the turbine. In addition, there are also multiple bleed flows with different pressure levels coming from the compressor. The sum of these bleed flows is named \dot{m}_B . Since only one mass flow \dot{m}_{Out} leaves the turbine, the exhaust mass flow can be calculated with the following equation.

$$\dot{m}_{Out} = \dot{m}_{FG} + \dot{m}_B \quad (5-6)$$

Since the compressor and the turbine sit on the same shaft, their rotational speed is equal. The rotational speed of the shaft is set to 6608 1/min [35]. Therefore, a change in power generation only results in a change in torque, not a change in rotational speed.

5.2.6 Modeling of the turbine in Epsilon Professional

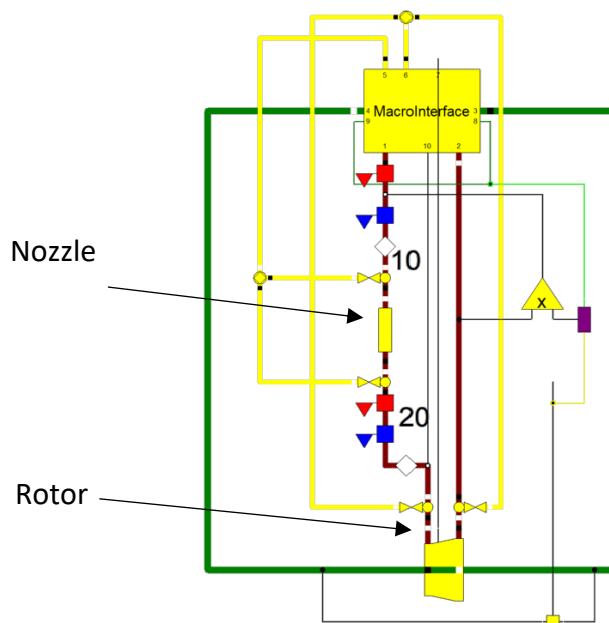
The turbine of the SGT-800 (57 MW) consists of three stages [36]. Each of these three stages is modeled separately. As explained, the turbine model sets the pressure level for its inlet flow. Therefore it defines the target pressure level for the compressor. The following figure shows the implementation of the turbine model in Epsilon Professional.



5-7: Implementation of the turbine

The central controller aims to raise the turbine's generated power to meet the target pressure level defined by the TMAP block. The TMAP block uses the ellipse law for calculating the normalized corrected mass flow. The pressure is then regulated so that the normalized corrected mass flow is one. [38] This model assumes that each turbine stage produces the same amount of power. Therefore the controller will raise or decline the generated power for each turbine stage based on the target pressure level. The higher the target pressure, the higher the generated power by each turbine stage.

The turbine stage model differentiates between the stator and the rotor. The nozzle is modeled as pressure drop (Comp 13) and the rotor is modeled with the turbine component (Comp 6) in Epsilon Professional. Each nozzle has two tap streams. One is in front of the nozzle, and one is behind. These tap streams are cooling streams for the stator blades. The modeling of a turbine stage is shown in the following figure.

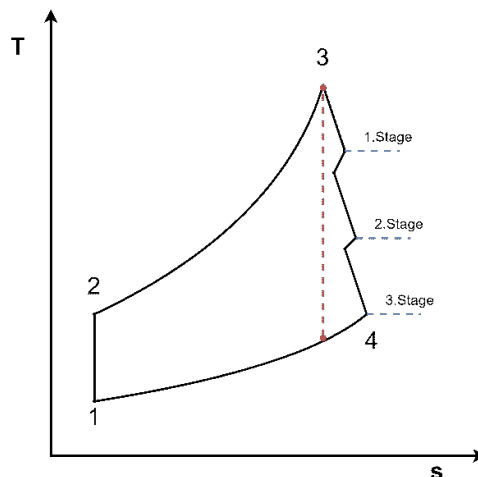


5-8: Implementation of a turbine stage

The turbine itself calculates the inlet pressure for the first turbine stage. Therefore the inlet and exit pressure of the turbine is known. This model assumes that each turbine stage generates the same amount of power [39]. To achieve this, a controller for each turbine stage regulates the outlet pressure of its stage. As a result, the inlet and outlet pressure levels for each turbine stage are defined. Just because the power generation is the same for each turbine stage, this does not mean this is also true for the pressure drop.

In addition, the isentropic efficiency for each turbine stage and, therefore the whole turbine must be considered. This isentropic efficiency does vary for different operating points. For the calculation of the isentropic efficiency, it is necessary to calculate the isentropic power generated by the turbine. Since the turbine has multiple stages and bleed flows, this is not as simple as assuming an isentropic expansion for the entire pressure drop. This is because the bleed flow gets mixed up with the flue gas. The entropy and the temperature of the bleed flows are lower compared to the flue gas.

It results in an overall decrease in entropy and temperature for the mixed gas compared to the flue gas [40]. This can be seen in the following diagram.



5-9: Ideal expansion compared to real expansion

Therefore the bleed flows have to be considered. To solve this problem, the isentropic power is calculated for each turbine stage. These isentropic stage powers are then added up. The result is the isentropic power generated by the whole turbine. With this approach, it would be possible for a perfect turbine to reach the calculated isentropic power.

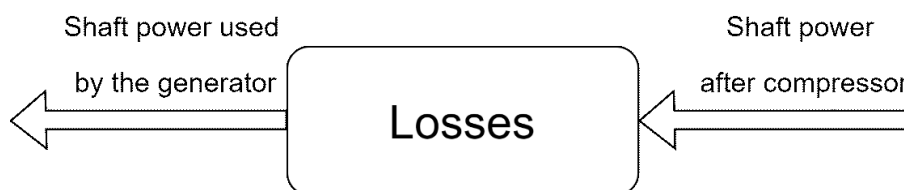
For the Validation and Hydrogen Run, the exhaust temperature of the flue gas and the isentropic efficiency of the turbine are predicted by regressions. This is not possible for the Reference Run. A values transmitter (Comp 36) is used to cope with this problem. This value transmitter aims to define the exhaust temperature of the flue gas. The higher this

temperature, the lower the efficiency of the turbine. The value transmitter uses the correction curve model as a reference. Therefore it measures the flue gas exhaust temperature of the correction curve model and transmits this value to the physical model. This value transmitter is only active for the Reference Run.

The controller, which sets the turbine's predicted exhaust temperature, works against the turbine's pressure controller, which changes the generated power for each stage to fit the pressure level. The reason for this is that a lower isentropic efficiency of the turbine results in a lower power generation by the turbine. Therefore, Epsilon Professional has to find an operation point for the turbine where both parameters are satisfied.

5.2.7 Modeling concept of the mechanical losses

This component aims to model mechanical losses. These losses represent, for example, friction losses that occur during power generation. The schematic of this component looks like the following.



5-10: Schematic function of the loss block

This component gets the shaft power P_{Shaft} behind the compressor as input. This power is the turbine's generated power P_{Turb} minus the power consumption of the compressor P_{Comp} .

$$P_{Shaft} = P_{Turb} - P_{Comp} \quad (5-7)$$

Therefore this component has to predict the power losses P_{Losses} for calculating the remaining power P_{Gen} that reaches the generator. This power can be calculated as follows.

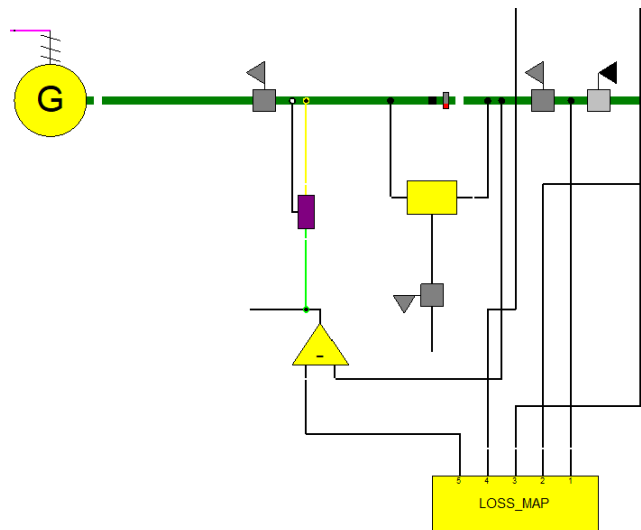
$$P_{Gen} = P_{Shaft} - P_{Losses} \quad (5-8)$$

Since these losses should not be too high, the result of this component should not have a high impact.

5.2.8 Modeling of the mechanical losses in Epsilon Professional

This component aims to predict a variety of mechanical losses. For the Reference Run, the loss is calculated by subtracting the shaft power of the generator from the shaft power coming

from the compressor. For the other runs, these losses are predicted by a regression. These predicted losses are subtracted from the shaft power after the compressor. For this operation, the calculator component (Comp 77) is used. This calculator component has logical lines as input. With the first line, it gabs the value of the shaft power after the compressor, and with the second line, it gabs the predicted loss. The so-calculated shaft power for the generator is then adjusted by a controller component (Comp 12). The following illustration shows the implemented loss model.

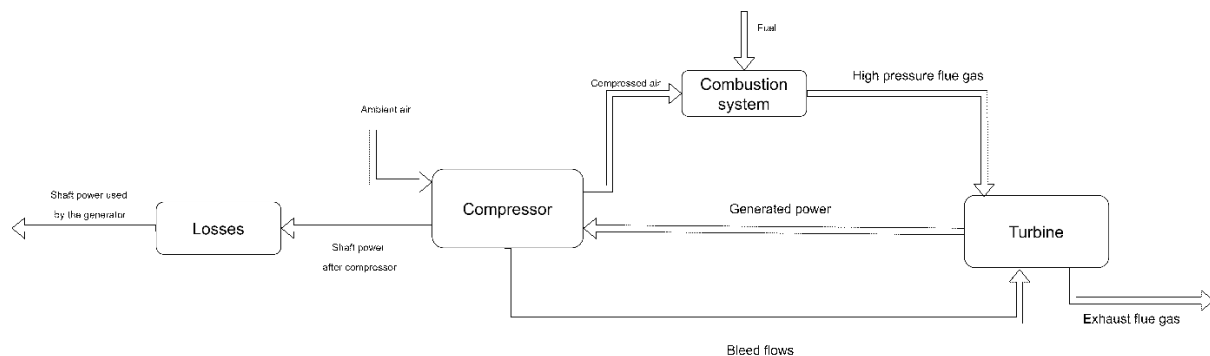


5-11: Implementation of the loss map in Epsilon Professional

The regression which predicts the loss is represented by the LOSS_MAP block. The exact creation of the regression will be explained later.

5.2.9 The complete gas turbine model in Epsilon Professional

In the preview subsections, each component of the gas turbine model was explained in detail. These four components are combined into the complete gas turbine model. The combined model looks like this.



5-12: All blocks combined to turbine model

Since each of these major components uses a regression to model the component's behavior, it is necessary to make a Reference Run. As explained earlier, this Reference Run aims to generate data for fitting these regressions. The way this Reference Run is going to be calculated is to use the correction curve model as a reference. Therefore all major flow characteristics in and out of the gas turbine model are transferred from the correction curve model. For the compressor, the air mass flow is transmitted. This is also true for the fuel mass flow in the combustion chamber. In addition, the turbine's generated electricity and the exhaust flue gas temperature are also transmitted. With these values defined, it is possible to calculate the gas turbine model. Therefore it is possible to generate operational data on the gas turbine. This data is needed to fit the multiple regressions used in the stand-alone version of the gas turbine model.

5.3 Design and Off-design calculation

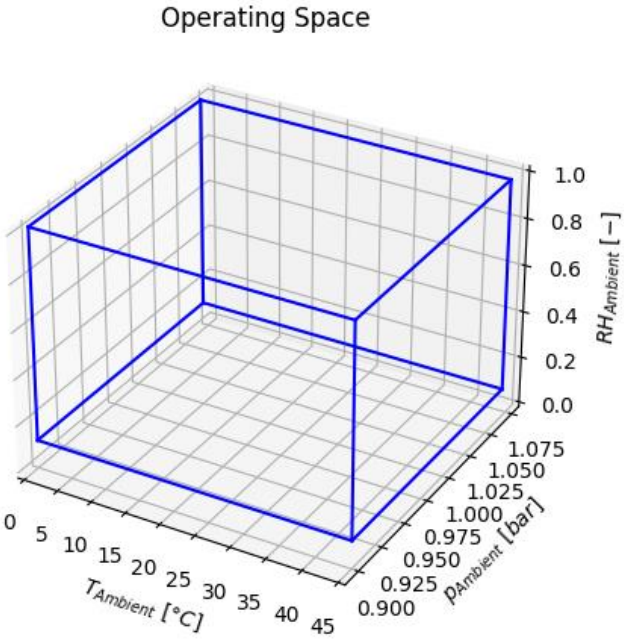
In Epsilon Professional there are two calculation modes. These modes are the design and the off-design calculation mode. [12] The design mode aims to calculate the dimensions of the components needed to meet the demanded requirements. The design calculation for a component is executed for one specific scenario. Therefore, this design calculation often takes place under reference conditions. [41] The ISO reference temperature is 288.15 K, the pressure is 1.013 bar, and the humidity is 0.6 [42, 43]. Therefore the whole turbine design is calculated to satisfy the given requirement and these conditions. One example of a design calculation in this model is the mass flow in the compressor. This mass flow is set in the design calculation. It is used as a reference in the off-design calculations for predicting the compressor's performance.

The off-design calculation does not change any design parameter of the model. The calculation is used to calculate the behavior of the design model under different conditions without making any design changes [41]. For the turbine model, this means that it is possible to calculate the turbine's behavior based on different ambient conditions. This calculation is used for the Reference, Validation and Hydrogen Run. Therefore the turbine model gets solved thousands of times for different scenarios. Each scenario has three input parameters. These parameters are the surrounding temperature, pressure, and humidity. Since the off-design calculation aims to map the behavior of the turbine, it is necessary to calculate as many different variations of these three input parameters as possible. The range of these parameters is as follows.

Table 5: Ambient parameters and their limits

Parameter	Min	Max
Temperature [K]	273.15	318.15
Pressure [bar]	0.90	1.07
Humidity [-]	0.1	1

These three parameters can be seen as a three-dimensional coordinate system. Therefore, it is necessary to calculate as many points in this three-dimensional coordinate system as possible. Since each of these parameters has its limits, this results in the three-dimensional operating space of the gas turbine. Every point calculated for this turbine model has to be within this defined space.



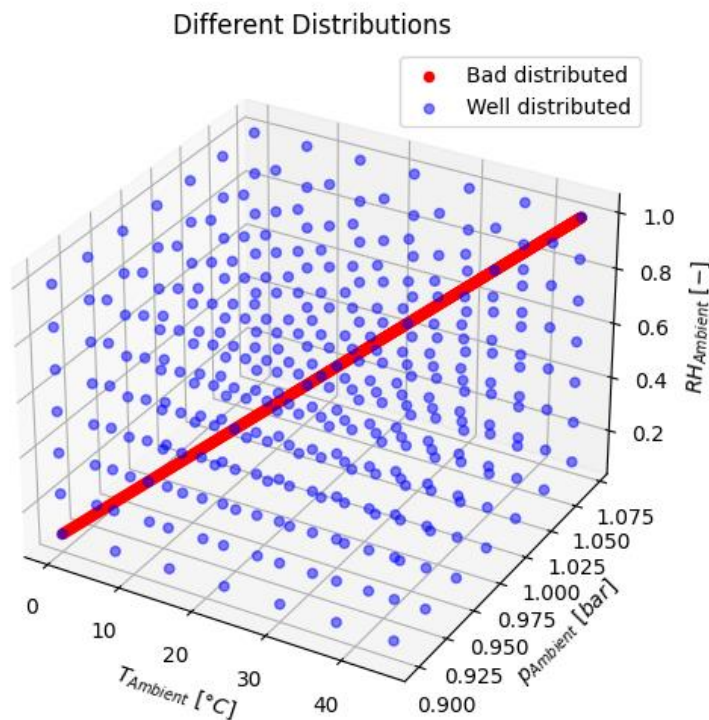
5-13: Operating space of the turbine model

Since the computation power is limited, it is essential to consider what scenarios are calculated. The mapping should be equally distributed in this three-dimensional space to avoid gaps in the representation. If this is not the case, specific areas may not be adequately represented. This is an essential factor if the so generated data is used for fitting the regressions used in the physical model. This is because if specific areas are not represented properly, this could result in a higher than expected error for the predictions of the regressions.

To cope with this problem, a monte carlo simulation is used. This monte carlo simulation generates 10976 scenarios. Each scenario is defined by a combination of the three ambient parameters. All these parameters have to be within the defined operating space. Each of these scenarios is then solved to generate data. This data is then used for fitting the regressions.

With this number of operation points, it is not easy to validate if the whole operating space of the turbine is properly covered. The assumption is that if each of these three parameters is equally distributed within its limits and appears random to each other, the whole space will be represented equally. Therefore each parameter will be checked individually and compared to the other parameters. It is important to check if these parameters appear random to each other because even if every parameter is distributed perfectly within its limits, this is not a guarantee that the whole operating space is covered.

One example can be seen in the following plot. All three parameters are perfectly distributed within their limits, but the parameters got paired by rising values. The red line represents this the worst possible distribution, while the blue dots represent the best possible distribution.



5-14: Comparison of distributions

This shows that the red line only covers a fraction of the operating space. Therefore it is not only necessary to validate that each parameter is equally distributed within its limits, but they also should appear random to each other. Therefore there should be no pattern visible if the parameters get plotted to each other. Even if one of these three parameters appears random to another parameter, this does not guarantee that this is true for the third one. Therefore

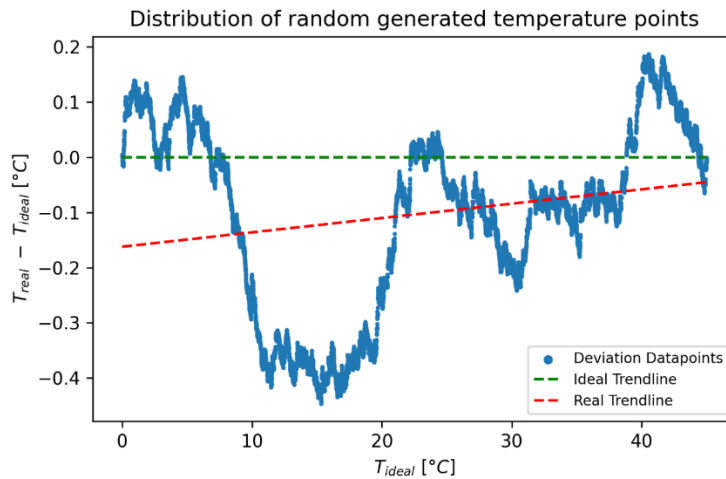
each of these three parameters has to be random to each other. Therefore the validation of the generated data is as follows:

1. Validate an equal distribution within the limit of each parameter
2. Validate if each parameter appears randomly to the other parameters

First, the ambient temperature is going to be validated. The temperature will be sorted by increasing values. The green line in the following plot represents an ideal distribution. The green line is generated with the following formula:

$$T = \frac{T_{max} - T_{min}}{n} \cdot x + T_{min} \quad (5-9)$$

In this formula, n is the number of data points shown in the plot, and x is the number of a specific data point. T represents the expected temperature at a given data point x for the n sorted temperature points. As a result, each deviation of this green line represents a variance from a perfect distribution within the given limits T_{max} and T_{min} .



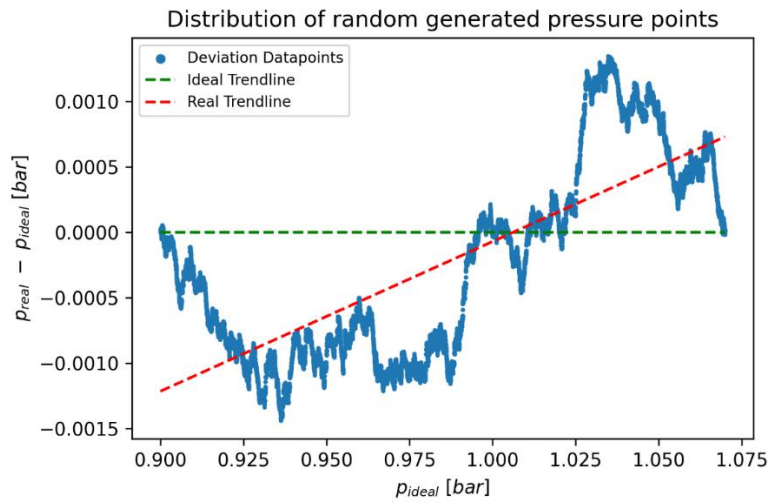
5-15: Distribution of the used ambient temperature values

The red line represent the trend line of the generated data points. As it is possible to see, there is no relevant deviation from an ideal distribution.

The values of the ambient pressure will be validated in the same way as the temperature. The green line will also represent an ideal distribution. For the green line, the following formula was used:

$$p = \frac{p_{max} - p_{min}}{n} \cdot x + p_{min} \quad (5-10)$$

The variable x represents the number of a specific data point, and n represents the total number of data points used. This formula can only be used if the data points get sorted by value. Therefore all values in the following plot are sorted.



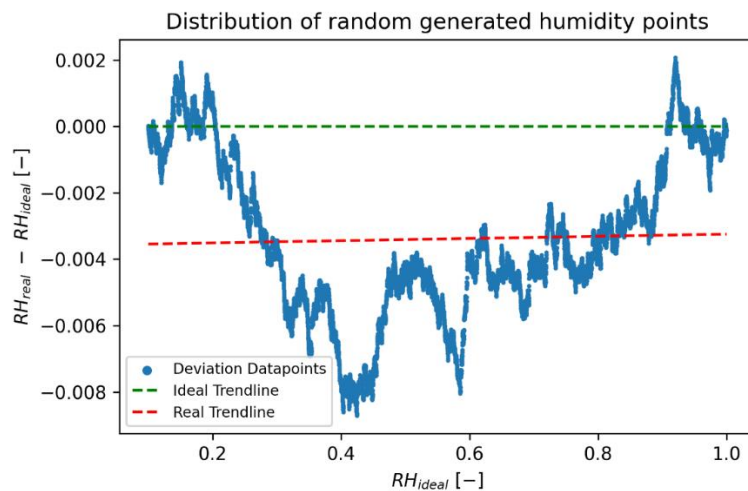
5-16: Distribution of the used ambient pressure values

This plot shows that there is no major deviation between these two lines. Therefore the generated points for the ambient pressure can be assumed to be equally distributed.

The data points of the ambient humidity also get sorted by value and plotted against a green reference line. This green line represents an ideal distribution within the given limits. For the reference line following formula was used:

$$RH = \frac{RH_{max} - RH_{min}}{n} \cdot x + RH_{min} \tag{5-11}$$

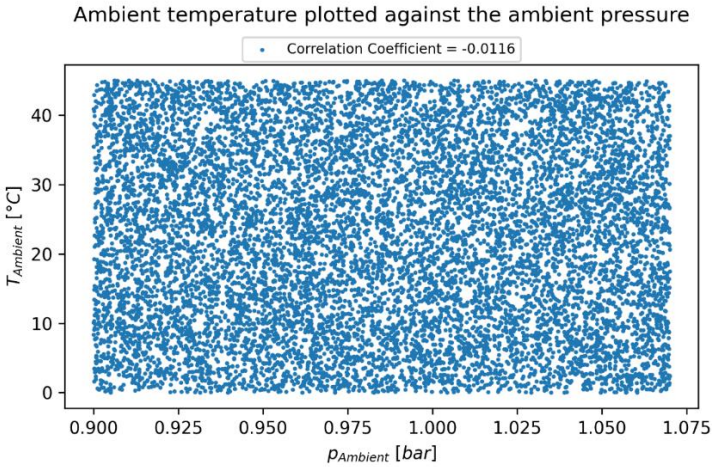
The variables n and x have the same meaning as in the previous functions.



5-17: Distribution of the used ambient humidity values

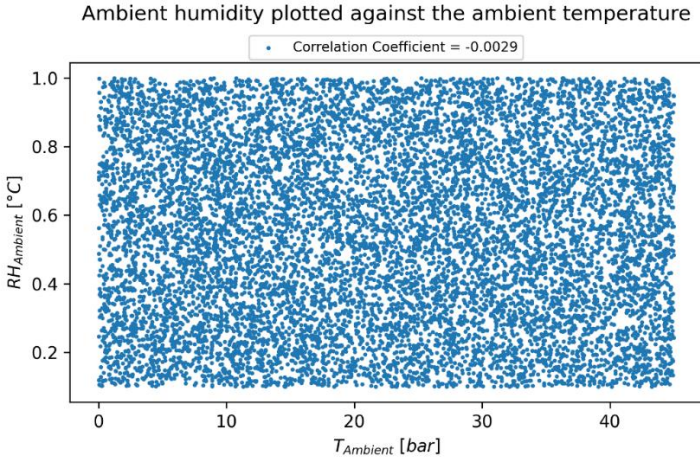
Since there is no major deviation of the ideal line, the ambient humidity can be assumed to be equally distributed.

As a result, each of these three parameters is equally distributed within their given limits. As shown in the example earlier, this does not guarantee that the whole operating space is covered evenly. Another important aspect is to validate if all parameters are random to each other. If this is not true major spaces could be missed in the Reference Run. To validate this, each parameter will be plotted against each other. This results in three plots. If there is no pattern of any kind in this plot, it will be assumed that these parameters are random to each other. If this is true, the operation space of the turbine is assumed to be covered. The ambient temperature is plotted against the ambient pressure in the following plot.



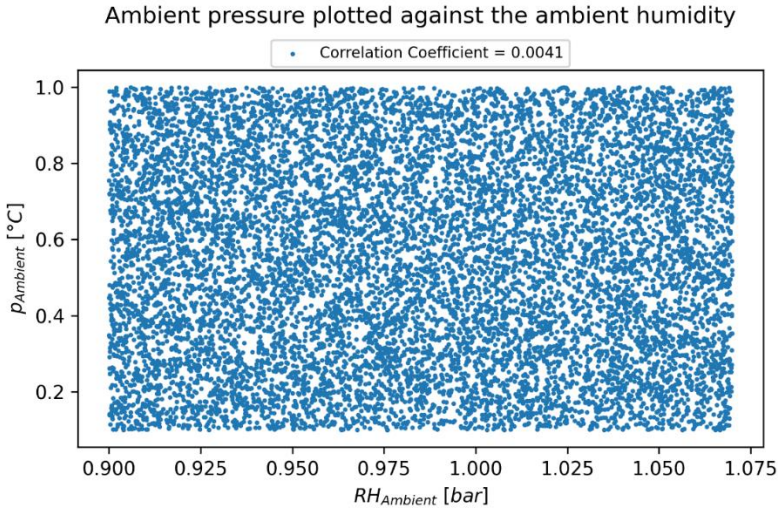
5-18: Representation of the correlation between the ambient pressure and temperature

As it is possible to see, there is no visible pattern or trend between these two points. Therefore these two parameters are assumed to be independent of each other. At this point, it is not safe to say that none of these two parameters correlates with the ambient humidity. Therefore it is necessary to check if these two parameters are also independent of the ambient humidity. The following plot will show the ambient humidity plotted against the ambient temperature.



5-19: Representation of the correlation between the ambient temperature and humidity

As it is possible to see, there is no visible pattern or correlation between the ambient temperature and the ambient humidity. The last step is to check if there is a correlation between the ambient pressure and the ambient humidity. These two parameters are plotted in the following diagram.



5-20: Representation of the correlation between the ambient humidity and pressure

This plot also shows no visible correlation between these two parameters. It was shown that the distribution of each parameter between the given limits is evenly, and no correlation exists between these three parameters. Therefore, it is assumed that the operation space is covered evenly by the generated operating points. As a result, it is possible to use these data points for the Reference Run. The data generated by the Reference Run is used to fit the regressions used in the physical model.

5.4 Calculation of the Reference Run

Each model takes about 30 seconds to solve on a laptop (Lenovo Thinkpad L15). Therefore calculating these 10 976 scenarios would take around four days. Gladly the ENEXSA GmbH provided access to their distributed calculation service which reduced the calculating time to around 1 h. This was the only reason why it was possible to calculate this many scenarios. Since the Reference Run is an off-design calculation, it is crucial that a design calculation was made before.

The Reference Run aims to generate data for fitting the regressions in the physical gas turbine model. Since these regressions are not active for the Reference Run, these values are taken from the correction curve model. These values are the air mass flow of the compressor inlet, the fuel mass flows into the combustion chamber, the exhaust temperature of the gas turbine, and the generated electric power of the generator. With this data from the correction curve model, it is possible to calculate these 10 976 defined scenarios. The regressions that will be fitted with this data are multivariant polynomial regressions. This type of regression will be explained in the next chapter.

5.4.1 Multivariant polynomial regressions

While a polynomial regression has only one input variable, a multivariant polynomial regression has multiple input variables. Therefore a multivariant polynomial regression also includes all interactions for a given order of all defined input variables. To illustrate the difference between these two regressions, the general formulations for both types are shown.

The following formula shows the general formulation of a quadratic polynomial [44].

$$f(x) = a \cdot x^2 + b \cdot x + c \quad (5-12)$$

Compared to this, the multivariant quadratic polynomial with two input variables has the following general expression [44].

$$f(x, y) = a \cdot x^2 + b \cdot x \cdot y + c \cdot y^2 + d \cdot x + e \cdot y + f \quad (5-13)$$

As it is possible to see, this regression does not only include all given orders for the variables but also all possible interactions between these variables. Therefore, the number of terms drastically rises with a higher polynomial order or a higher number of input parameters.

This figure shows a graphical representation of all terms for a third-order multivariant polynomial regression with three variables.



5-21: Graphical representation of all terms for a multivariate regression with three input parameters

It is possible to calculate the number of all terms for a given order and a given number of input variables. The number of all terms up to a given order including all cross terms can be calculated with the formula (5-14) [45]. In this formula n is the number of input variables and m is the highest order of the polynomial.

$$s(m, n) = \binom{m+n}{n} = \frac{(m+n)!}{n! \cdot (m-n+n)!} \quad (5-14)$$

$$s(m, n) = \frac{(m+n)!}{n! \cdot m!} \quad (5-15)$$

This shows that the number of terms rises drastically if the number of input variables or the highest order of the polynomial increases. This is important to consider when using multivariate polynomial regressions.

5.4.2 Multivariate polynomial regression of the compressor

The air mass flow of the compressor must be very accurate because it represents the main mass flow on the turbine. Therefore, slight deviations in the air flow compared to the correction curve model can significantly impact the accuracy of the results. One aspect that makes the compressor's modeling easier is the fuel's independence. Since the rotational speed is constant with 6608 1/min and the compressor does not interact with the flue gas.

It is important to consider that the variation in the generated power by the gas turbine does not mean there is a change in the rotational speed. The cause of the power variation is based on the change in torque. Therefore, the compressor can have the same rotational speed for every ambient condition. The compressor also does not interact with the flue gas. Therefore,

it is not dependent on the fuel used. This makes it possible to use the ambient conditions as parameters for predicting the air mass flow. These parameters are ambient temperature, pressure, and humidity. The regression can be written as follows.

$$m_{In} = f(T_{Ambient}, p_{Ambient}, RH_{Ambient}) \quad (5-16)$$

The type of regression which will be used is a multivariate polynomial regression. As explained earlier, this type of regression uses polynomials for each input parameter and considers all cross terms. Since it is necessary to create a high accuracy for this mass flow prediction, a high polynomial degree is used. For this regression, a maximum polynomial degree of six is used. With this formula, it is possible to calculate the number of terms this regression will have.

$$s(m, n) = \frac{(n + m)!}{m! \cdot n!} \quad (5-17)$$

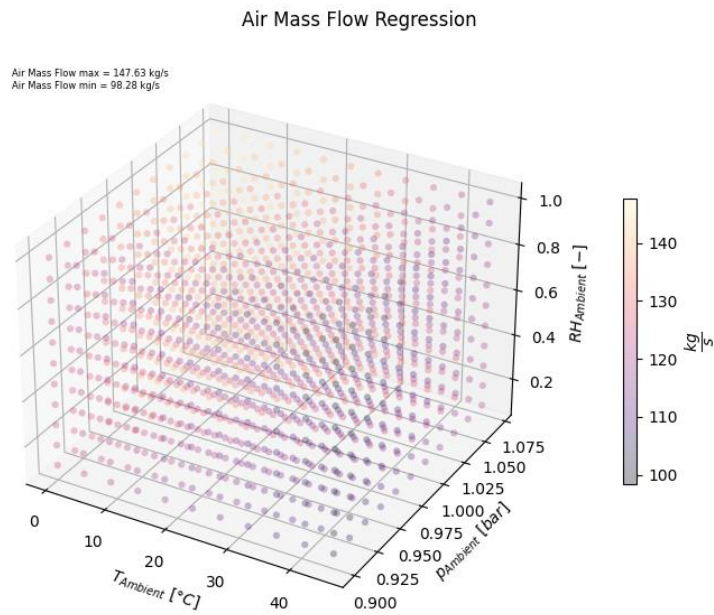
In this formula, n is equal to the number of input parameters which is three in this case. The parameter m is equal to the maximum order of the polynomial and, therefore six.

$$n = 3$$

$$m = 6$$

$$s(6, 3) = \frac{(6 + 3)!}{6! \cdot 3!} = 84$$

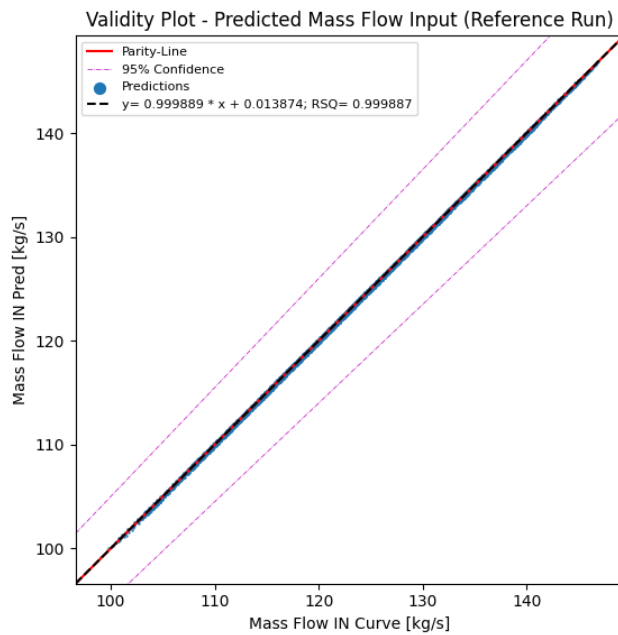
It shows that the regression will have 84 terms which is extremely large. This is acceptable because this regression will not be used for extrapolation and is only used on the interval it was created on. To ensure no hidden spikes, the regression was calculated for a large amount of different ambient conditions. The result is shown in the following plot.



5-22: Air mass flow for multiple scenarios

This plot indicates that there are no hidden spikes. The reason for this assumption is that the minimum and the maximum values are in an expected range. In addition to this, the plot also shows a clear color shift within the operating space.

Even though this plot shows that the regression is behaving as expected, it says nothing about its accuracy. Therefore the regression is used for predicting the data it was fitted on. The accuracy of this regression for the used data can be seen in the following plot.



5-23: Validation of the air mass flow

As it is possible to see, the regression is very accurate. This regression will not be used for extrapolation therefore, the high number of terms should not be a problem. Another important aspect of this regression is that it only uses predefined parameters as input. This is important for the numerical behavior of the model. Since these parameters are constant throughout all iterations, the regression can instantly predict the “right” air mass flow. Therefore the air mass flow in the compressor does not change while the model gets calculated. This makes the gas turbine model much more stable and results in a more reliable and faster model. Since multiple regressions constantly predict values based on changing input parameters, having one regression that can instantly predict an important parameter makes a huge difference.

5.4.3 Defining a multivariant polynomial regression for the combustion

The fuel control system aims to set the fuel mass flow. The problem, in this case, is that the fuel system has to work not only for methane but also for hydrogen. Since methane and hydrogen do not have the same heating value, the mass flow will likely differ significantly. This also has an impact on the predicted parameter. The prediction of the fuel mass flow would only be a valid option if there were no fuel changes. Since the fuel will be changed from methane to hydrogen this is not an option. Another critical point is that the amount of fuel influences the firing temperature, which changes the isentropic efficiency of the turbine. Therefore, it is likely that the results of the combustion system will influence the turbine efficiency.

The fuel control system will use the expansion ratio *EXPR* and the normalized corrected speed *NCSPD* of the turbine as input parameters for predicting the exhaust temperature of the gas turbine.

$$T_{ex} = F(EXPR, NCSPD) \quad (5-18)$$

To control the exhaust temperature of the turbine, the fuel control system will regulate the mass flow of fuel. This makes it possible to regulate the mass flow for different fuel types.

There is only one drawback with this approach. The exhaust temperature depends on the turbine's isentropic efficiency, and the isentropic efficiency depends on the fuel mass flow. Since the exhaust temperature is the primary reference variable for the fuel mass flow regulation, this approach must be taken cautiously.

Another aspect is that the composition of the flue gas changes with the fuel. Therefore, the expansion behavior and temperature drop through the turbine can differ for methane and hydrogen. As a result, the energy input of the fuel for a given scenario is highly dependent on the fuel used. Therefore, it is safe to say that not only will the mass flow of the fuel change if the fuel gets changed from methane to hydrogen, but also the energy input will change.

Since this regression will interact with the turbine's isentropic efficiency, the polynomial degree is an important parameter for not risking a runaway situation. Therefore, the maximum polynomial degree used is two. Since the number of input parameters and the maximum polynomial degree are known, it is possible to calculate the number of terms used in this regression.

$$s(m, n) = \frac{(n + m)!}{m! \cdot n!} \quad (5-19)$$

$$n = 2$$

$$m = 2$$

$$s(2, 2) = \frac{(2 + 2)!}{2! \cdot 2!} = \frac{4 \cdot 3 \cdot 2 \cdot 1}{2 \cdot 1 \cdot 2 \cdot 1} = 6$$

This regression only uses six terms. Therefore, the threat of overfitting should not be a problem. The base formula of this multivariant polynomial regression with two parameters and a maximal order of two looks as follows.

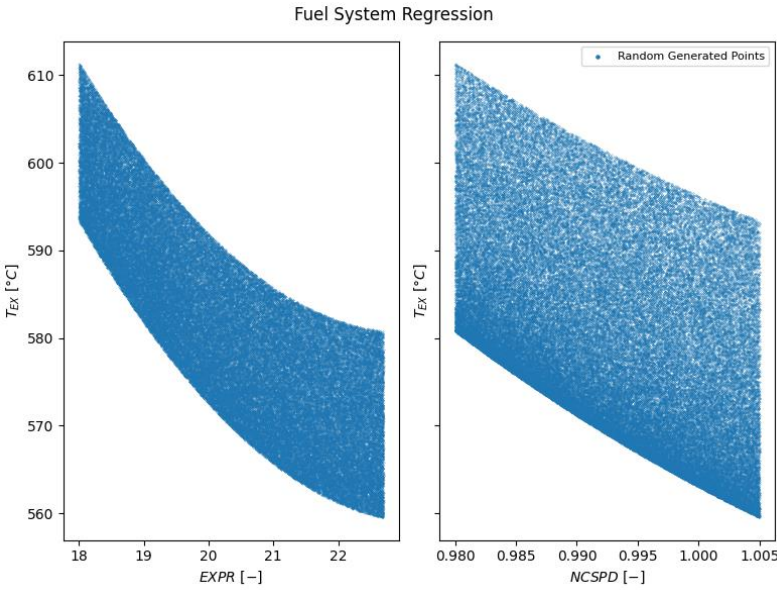
$$T_{ex} = A + B \cdot EXPR + C \cdot NCSPD + D \cdot EXPR^2 + E \cdot EXPR \cdot NCSPD + F \cdot NCSPD^2 \quad (5-20)$$

Therefore, six coefficients are fitted by the data calculated in the Reference Run. The values of the fitted coefficients are based on around 10976 data points and are shown in the following table.

Table 6: Coefficients of the fuel system regression

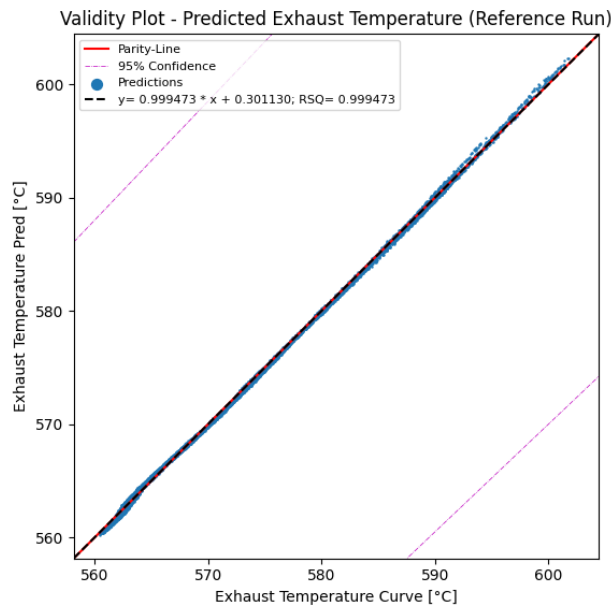
Coefficient	A	B	C	D	E	F
Value	8740.7841	-28.0565	-14946.5626	1.1921	-27.5279	7416.2836

Since the maximum regression order is limited to two, there should be no unexpected spikes in the regression. If this regression had a higher order, there could be a risk of hidden spikes between the data points used for the regression. In this case, the regression would behave perfectly fine when used on known data points, but it could produce large deviations on new data. This behavior would be an example of an overfitted function. Since this regression is based on 10976 data points and uses only six terms, this should not be a problem. This regression was calculated for a variety of new data points. The result is shown in the following two plots.



5-24: Operating space of the fuel system regression

These plots show that the regression has no hidden spikes and no strange or unexpected behavior is visible. To verify the accuracy of the regression, it will be used to predict the exhaust temperature of the turbine based on the normalized corrected speed and the expansion ratio. This predicted exhaust temperature is then plotted against the given exhaust temperature of the correction curve model. This is done for all 10976 data points. In addition to this, the mean accuracy is also calculated. The plot and the calculated accuracy are shown in the following plot.

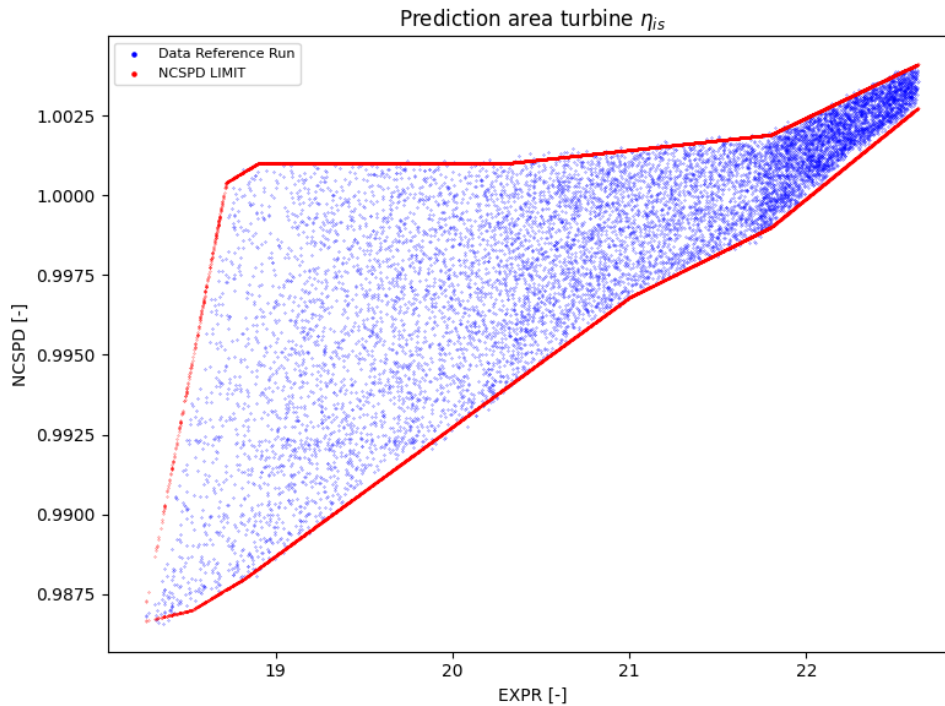


5-25: Validation of the exhaust temperature

This plot shows that the regression has high accuracy and can be used to control the fuel mass flow.

5.4.4 Narrowing down the combustion regression

Predicting the fuel mass flow is essential for this simulation and its numerical behavior. Since the Validation Run will deviate from the Hydrogen Run, the regression will be narrowed down by multiple other functions. The reason for this is to avoid extrapolation. This has to be avoided because this regression strongly interacts with the prediction for the isentropic efficiency. Therefore every extrapolation in the fuel mass flow prediction of the combustion system would result in a possible extrapolation in the prediction of the isentropic efficiency of the turbine. With two extrapolating regressions, the impact on the results could be very strong. To avoid this, the prediction area of the fuel control system is narrowed down. The way this is done is illustrated in the following plot. In this plot, the turbine expansion ratio is on the x-axis and the normalized corrected speed of the turbines inlet is on the y-axis.



5-26: Operating area of the regression

This plot shows that the data points generated by the Reference run are a distinct closed area. This area includes all data points the regression uses for its predictions. Multiple linear functions will narrow down this area to avoid extrapolation for this function. The expansion ratio will not be influenced by any kind because it will not likely vary much. Since this regression will also be used for the hydrogen prediction, the normalized corrected speed will likely vary. Therefore it is going to be narrowed down. A minimal and maximal limit for both parameters is defined to achieve this. The minimal and maximal limit for the normalized corrected speed is predicted by multiple functions depending on the expansion ratio of the turbine. Therefore, the limits used for the normalized corrected speed depend on the turbine's expansion ratio.

With these precautions, the numerical behavior of the model should be much more stable. The reason for this is that the normalized corrected speed is only going to vary in a known range. This makes it easier for the fuel system to predict the right amount of fuel.

1.1.1 Defining a multivariant polynomial regression for the turbine

One important aspect is predicting the isentropic efficiency based on the normalized corrected speed and the expansion ratio. Since it is not known how each of these two parameters influences the isentropic efficiency, a multivariant polynomial regression is used.

The isentropic efficiency is calculated by dividing the actual power generation of the turbine by the ideal power generation. Since no turbine can realize an isentropic expansion, the generated power will always be lower than the ideal power generation. This non-ideal expansion also has other side effects than the power generated.

The isentropic efficiency also affects the exhaust temperature of the flue gas and, therefore the regression of the fuel control system. Since the isentropic efficiency of the turbine is modeled as a function of the expansion ratio and the normalized corrected speed, it depends on the firing temperature. There is also a good chance that the firing temperature will change slightly when changing the fuel from methane to hydrogen. Therefore, there is a good chance that this regression will extrapolate at least a bit. For this reason, it is impossible to use a higher degree polynomial for the regression. To cope with this problem, a new strategy is used. A piecewise linear approach is used. Therefore, the data generated by the Reference run is split into three separate intervals. The data points in each of these intervals get approximated by their linear regression. The so calculated regressions and the corresponding intervals are shown in the following. In the following equations the isentropic efficiency is represented by η_{is} .

1.Interval

$$EXPR < 20.1$$

$$\eta_{is_1} = 0.7678 + 0.0007 \cdot EXPR + 0.1226 \cdot NCSPD \quad (5-21)$$

2.Interval

$$20.1 \leq EXPR < 21.8$$

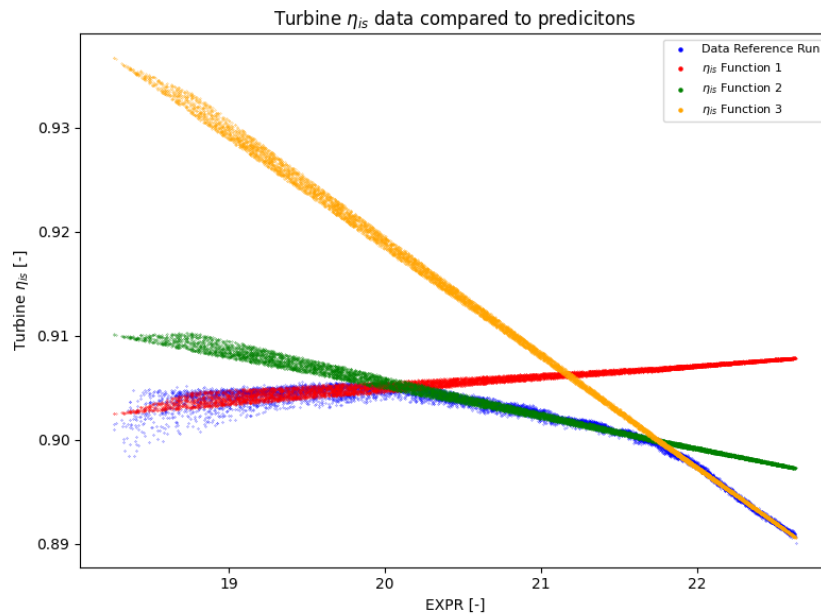
$$\eta_{is_2} = 0.8374 - 0.0035 \cdot EXPR + 0.1381 \cdot NCSPD \quad (5-22)$$

3.Interval

$$21.8 \leq EXPR$$

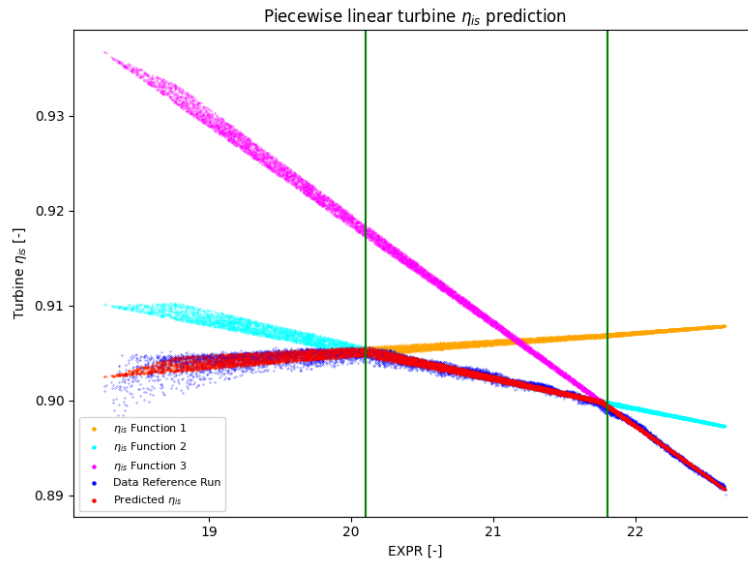
$$\eta_{is_3} = 0.9828 - 0.0112 \cdot EXPR + 0.1602 \cdot NCSPD \quad (5-23)$$

These functions can now be used for predicting the isentropic efficiency of the turbine. In the following plot, all three of these functions are shown for the whole interval.



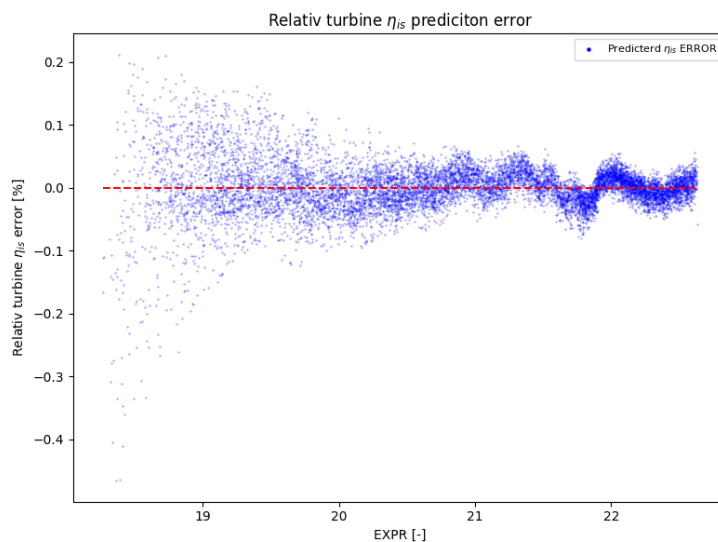
5-27: Representation of all used regressions

This plot shows that each function predicts a different isentropic efficiency for the turbine. Therefore, the model has to decide which of these values it will use. Since each regression is defined for a specific interval, the model could decide based on this interval. The problem with this approach is that the functions do not necessarily intersect at this point. Therefore, a gap between the functions would be the result. This gap could cause numerical problems. Therefore, this would not be a good solution for this problem. A better way of solving this is to always use the smallest of the predicted values. Therefore, each of these three regressions predicts one value and the model compares these values to each other. Subsequently, the smallest value is used. With this approach, the model only switches the regression it uses on intersections. Therefore, no gap could cause numerical problems. One problem with this approach is that the defined interval borders should be very close to the intersection between these functions. The reason for this is that each of these functions is only based on the data of its interval. Therefore, if the intersection of these functions is outside of the interval, it will extrapolate. This is not a significant problem in this case because all functions used are linear. Therefore, there is not a high risk with slight extrapolations.



5-28: All used regressions and the interval borders

As it is possible to see, the intersections are very close to the interval limits (green vertical lines) and should not cause more significant deviations. Even though the accuracy of each function is high, it is necessary to validate the accuracy of these functions combined. Therefore the approach of picking the smallest predicted value has to be validated. As a result, these piecewise linear regressions are used for predicting the isentropic efficiencies for all data points of the Reference Run. These predictions are used to calculate the percentual deviation from the correction curve model. This deviation is shown in the following plot.



5-29: Prediction error of the used regression

As it is possible to see the deviation is not very high and should therefore be capable of predicting the isentropic efficiency of the turbine based on the expansion ratio and the normalized corrected speed. This regressions prediction area will be narrowed down similarly

to the fuel control system. Therefore, these regressions only predict based on values of a defined area.

5.4.5 Defining a multivariant polynomial regression for the losses

The mechanical losses are going to be predicted by a regression. Therefore, it is necessary to define input parameters. These input parameters are the air mass flow in the compressor \dot{m}_A , the ambient temperature $T_{Ambient}$, and the shaft power after the compressor P_{Shaft} .

$$P_{Shaft \text{ for generator}} = F(\dot{m}_A, T_{Ambient}, P_{Shaft}) \quad (5-24)$$

As explained previously, the compressor predicts air mass flow and only depends on the ambient pressure, temperature, and humidity. Therefore, the ambient temperature and the compressor's inlet air mass flow do not depend on the fuel type.

Since this regression will be based on the data generated by the Reference Run this regression will likely be extrapolating a bit. The reason for this is that the power generation of the turbine could be highly dependent on the fuel used. Even though the ambient temperature and the air mass flow in the compressor are not dependent on the fuel used in the turbine, it can be assumed that the ratio between these three input parameters will vary with a fuel change. This would result in an extrapolation of this regression. Therefore the polynomial degree should not be too high for not to risk large deviations by slight extrapolations.

As a result, the maximal polynomial degree is limited to two. With three input parameters for this regression, the number of terms can be calculated as the following:

$$s(m, n) = \frac{(n + m)!}{m! \cdot n!} \quad (5-25)$$

$$n = 3 \quad (5-26)$$

$$m = 2 \quad (5-27)$$

$$s(2, 3) = \frac{(3 + 2)!}{3! \cdot 2!} = 10 \quad (5-28)$$

This shows that the regression will only have 10 terms and a maximum polynomial order of two. Therefore it should be possible for the regression to extrapolate a bit without creating a significant error. The base formula used for the regression looks like this:

$$\begin{aligned}
 LOSS = & A + B \cdot P_{Shaft} + C \cdot T_{Ambient} + D \cdot \dot{m}_A + E \cdot P_{Shaft}^2 + F \cdot P_{Shaft} \\
 & \cdot T_{Ambient} + G \cdot T_{Ambient}^2 + H \cdot T_{Ambient}^2 + I \cdot T_{Ambient} \cdot \dot{m}_A \quad (5-29) \\
 & + J \cdot \dot{m}_A^2
 \end{aligned}$$

All 10976 data points from the Reference Run are used to fit this formula. Since the number of terms in this formula is very low compared to the number of data points, overfitting should not be a problem. The coefficients of this formula can be seen in the following table.

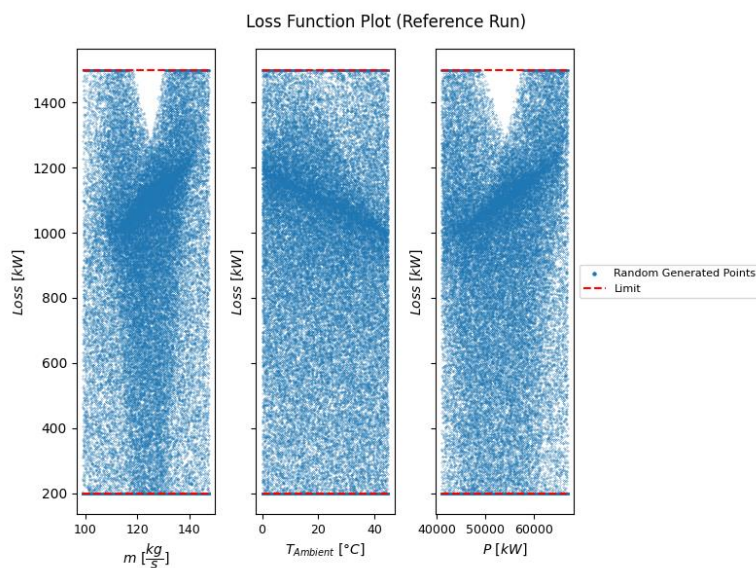
Table 7: First five coefficients of loss regression

Coefficient	A	B	C	D	E
Value	354.6941	-1.1249	-151.0631	519.5983	-1.4229

Table 8: Remaining coefficients of the loss regression

Coefficient	F	G	H	I	J
Value	0.0009	0.0212	0.3707	0.6907	-6.7009

In addition to the regression, the mechanical loss will have a lower limit of 200 kW and an upper limit of 1500 kW. To validate if this regression behaves as expected and has no hidden peaks in its defined area, it is calculated for different input parameters (all within their limit) and plotted in the following diagram.



5-30: Operating space of the loss map

This regression is limited from 200 kW to 1500 kW in Epsilon Professional. The reason for this is that with the fuel change to hydrogen there is a considerable risk of extrapolation, and with these limits, the error, should be relatively small, even in a worst-case scenario. Since no peaks are visible in the plot and the whole regression behaves as expected.

At this point, every regression is fitted with the data generated by the Reference Run. Therefore the physical model can work without the correction curve model. To validate the accuracy of the whole physical model, another run was executed with methane as fuel. This run is referred to as a Validation Run.

5.5 Calculation of the Validation Run

The Validation Run aims to see how accurate the regressions perform when they are all active. This is because the results of these regressions interact with each other. One example for this is the fuel mass flow. The higher the fuel mass flow the higher the firing temperature. This results in a higher normalized corrected speed. With a change in the normalized corrected speed, the isentropic efficiency of the turbine changes. Therefore, the exit temperature of the turbine changes. Since the fuel system uses the exit temperature of the turbine as a control variable, this also affects the fuel mass flow. Since these two regressions interact, this could cause numerical problems, or this behavior could result in multiple numeric stable alternative operating points. These operating points could depend on the start value used for the iteration. This would not be an acceptable result, because a gas turbine has only one way it reacts to given conditions. Therefore it is necessary to see if the gas turbine model can reliably produce good enough results compared to the correction curve model. For this run also, 10907 combinations of ambient conditions were generated. This was done with the same functions used as for the Reference Run. Since it was extensively shown that all scenarios are equally distributed over the whole operating space, this is also assumed for these 10907 newly generated operating points.

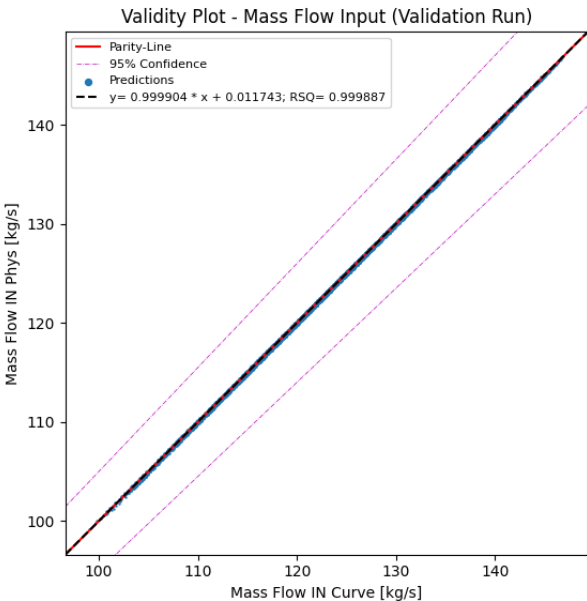
All these scenarios are calculated by the correction curve model and the gas turbine model. The results generated by these two models are then compared to each other. One aim of this comparison is to validate if the accuracy of the gas turbine model is nearly as high as the individual regressions themselves. The model's accuracy is expected to be slightly lower than the individual regressions, but it should not be much lower. The accuracy could drop rapidly because there could be multiple numerical stable results. Therefore it is essential to show that this is not the case.

If the gas turbine model can reliably produce similar results to the correction curve model, it is assumed that there are no alternative results the gas turbine model converges. Therefore the model should be able to cope with the fuel change from methane to hydrogen.

To verify this run all regressions are compared to the correction curve model. Therefore the air mass flow, the fuel mass flow, the exhaust temperature of the turbine and the generated electrical power will be compared. If these parameters are similar enough to the correction curve model, it will be assumed that the gas turbine model is a good representation of the real turbine.

5.5.1 Validation of the air mass flow

The air mass flow gets predicted by the regression used in the compressor module. Therefore, the air mass flow in the compressor should be nearly the same for the correction curve model and the gas turbine model. In the following plot, the air intake in the compressor of the correction curve model is on the x-axis and the air intake of the gas turbine model is on the y-axis. If the gas turbine model predicted the airflow perfectly, the plot would show every data point on the red reference line.

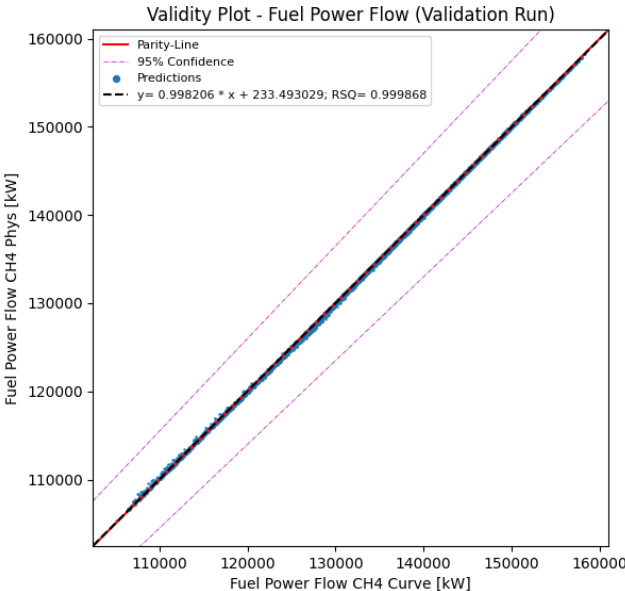


5-31: Validation of the air mass flow for new scenarios

As it is possible to see in this plot, the regression works with very high accuracy. This is expected because the regression only uses environmental parameters like the ambient temperature, the ambient pressure, and the ambient humidity as input parameters. Therefore it operates independently from other regressions.

5.5.2 Validation of the fuel power flow

The fuel directly flows in the combustion chamber and is controlled by the fuel control regression. This regression uses the expansion ratio and the normalized corrected speed to predict the turbine's exhaust temperature. To adjust this value, a controller changes the fuel power flow to match the predicted exhaust temperature of the turbine. If the fuel power flow of the gas turbine model deviates from the correction curve model, this could be either an error generated by the fuel control regression or the isentropic efficiency regression of the turbine. This is because these regressions strongly interact, as explained earlier. Therefore they can not be validated separately. In the following plot, the fuel power flow of the correction curve model is plotted against the fuel mass flow predicted by the fuel control system.

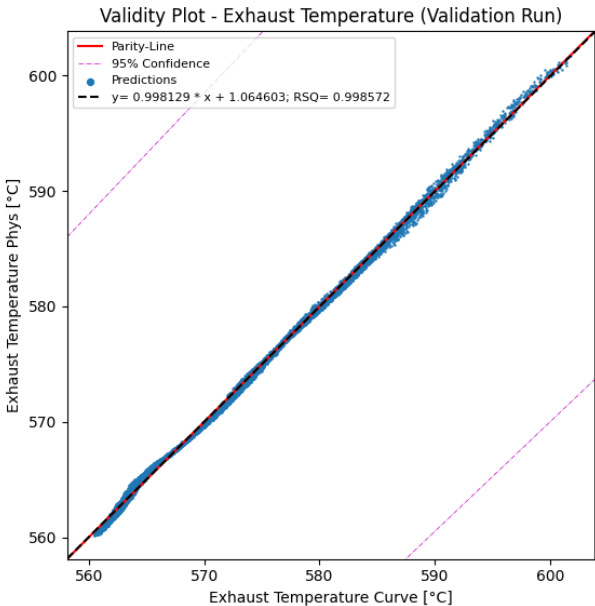


5-32: Validation of the fuel power flow for new scenarios

As it is possible to see the fuel control system works pretty accurately. It also indicates that the efficiency prediction of the turbine is also working correctly. This is because the exhaust temperature has to be suitable for the fuel control system to work. Since the environment defines parameters like the pressure and humidity of the exhaust flow, the temperature is the only variable controlled by the turbine efficiency. Therefore these two regressions have to work together to generate accurate results. Therefore if one regression produces accurate results, it indicates that the other is also working correctly.

5.5.3 Validation of the isentropic turbine efficiency

The isentropic efficiency is the first parameter that will be validated without being able to compare it directly to the correction curve model. Since the mass flow and the fuel flow were predicted quite accurately, it can be assumed that the firing temperature is very close to the expected one. As mentioned earlier, the environment predates exhaust pressure and humidity. Therefore it is possible to validate the regression for the isentropic turbine efficiency by the exhaust temperature. In the following, the exhaust temperature of the correction curve model is plotted on the x-axis, and the gas turbine model is on the y-axis.



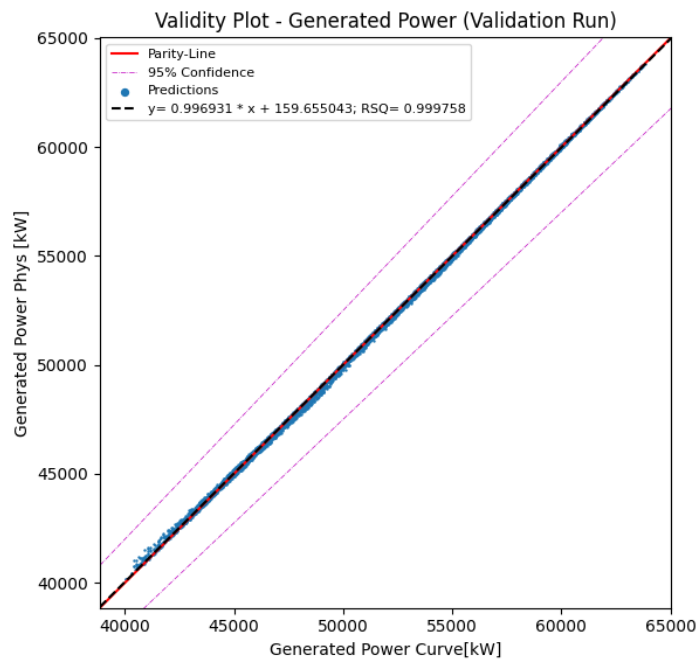
5-33: Plot of the exhaust temperature

This shows that also the exhaust temperature of the gas turbine model only has minor deviations from the correction curve model. If this is combined with the accuracy of the fuel system, it is safe to say that the interaction between the fuel system and the turbine efficiency works as accurately as expected.

5.5.4 Validation of the generated power

One of the most critical parameters of this gas turbine model is the generated electrical power. Therefore, it is crucial for this model to predict the generated power precisely. This parameter can be directly compared to the correction curve model. Since each regression was validated on its own and then when interacting with the other regression, the generated power should be nearly as accurate as the regressions used. An important aspect to consider is that the generated electrical power can only be correct if all regressions work together and do not create a too large error. Therefore if this parameter is close enough, it can be assumed

that the gas turbine model is working correctly. In the following plot, the generated electrical power of the correction curve model is on the x-axis and the generated electrical power of the gas turbine model is on the y-axis.



5-34: Validation of the power generation for new scenarios

Is it possible to see in this plot that these values are very close to each other. Therefore, the gas turbine model is working correctly.

After it was shown that each of these regressions can predict their parameter very accurately, it is now shown that they also work together and generate accurate results. Therefore, it can be assumed that the gas turbine model can simulate the behavior of the gas turbine. As a result, changing the fuel from methane to hydrogen should be possible, and the gas turbine model should produce valid results.

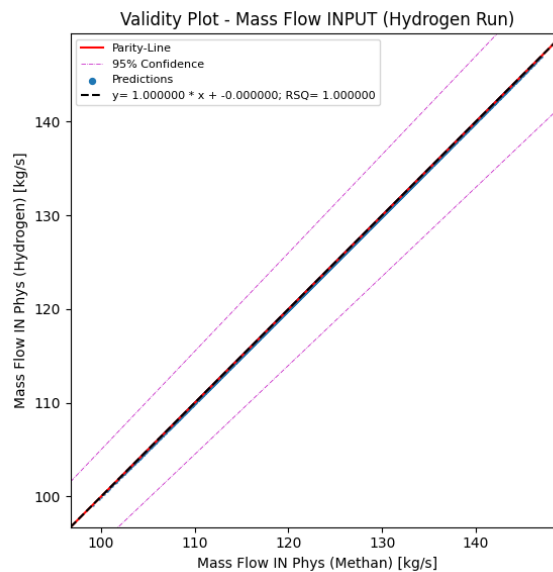
5.6 Calculation of the Hydrogen Run

The Hydrogen Run aims to see how the gas turbine reacts if the fuel changes from methane to hydrogen. The same ambient conditions are used for this run as in the Validation Run. This is because it allows a direct comparison between these two runs. It is important to note that this run's regressions are not changed. The only regression that will predict the same values for both runs is the regression predicting the air mass flow in the compressor. This regression is only dependent on the ambient conditions and, therefore not dependent on the fuel used.

The results of the Hydrogen Run will be compared to the results of the Validation Run. With this reference, it will be easier to see changes in the operational behavior of the gas turbine induced by the fuel change.

5.6.1 Air mass flow in the compressor

As indicated earlier, there should not be any change because the regression used for the mass flow in the compressor is not dependent on the fuel. Since the same environmental parameters are used, the regression should have the same result.

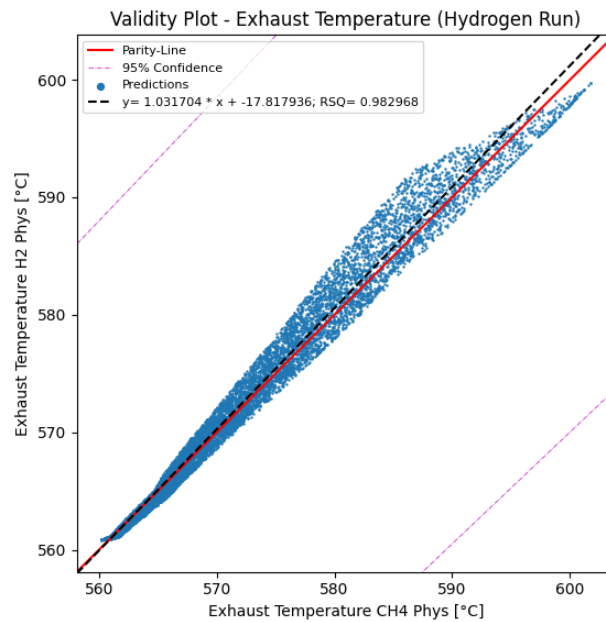


5-35: Comparison of the air mass flow

This plot shows that the regression predicts the same values in both runs. Therefore it works as expected. If there were deviations, this would indicate that the ambient parameters have changed. If this is true, then this would show that the wrong ambient conditions were used for the calculation. Since this did not happen, the Methane and Hydrogen Run are using the same operating points.

5.6.2 Exhaust temperature

The exhaust temperature shows no clear trend compared to the methane-fired gas turbine. In the following plot, the exhaust temperature of the Validation Run is on the x-axis, and the exhaust temperature of the Hydrogen Run is on the y-axis.

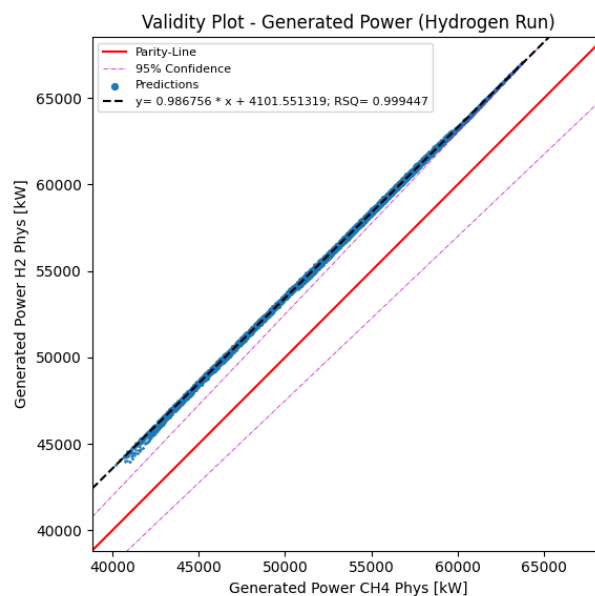


5-36: Comparison of the exhaust temperatures

This shows that the exhaust temperature of the hydrogen is sometimes lower and sometimes higher compared to methane. The trend line of the hydrogen shows that exhaust temperature is higher on average compared to methane.

5.6.3 Generated electrical power

The generated electrical power shows a much clearer trend than the exhaust temperature. The generated electrical power tends to be higher when switching from methane to hydrogen. This can be seen in the following plot.

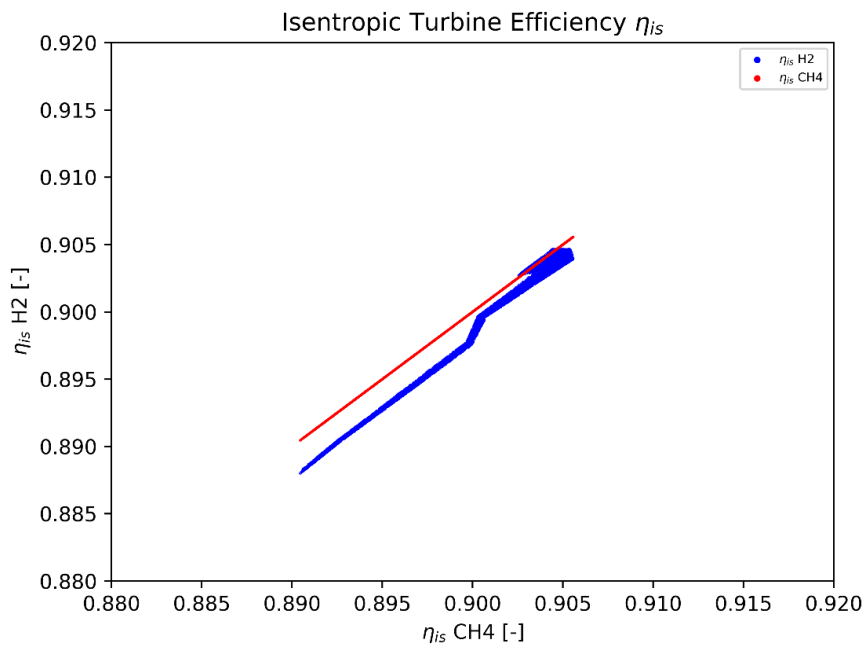


5-37: Comparison of the generated power

As this plot shows the generated electrical power is in all cases calculated higher when switching from methane to hydrogen. The mean power advantage is about 3 MW compared to methane.

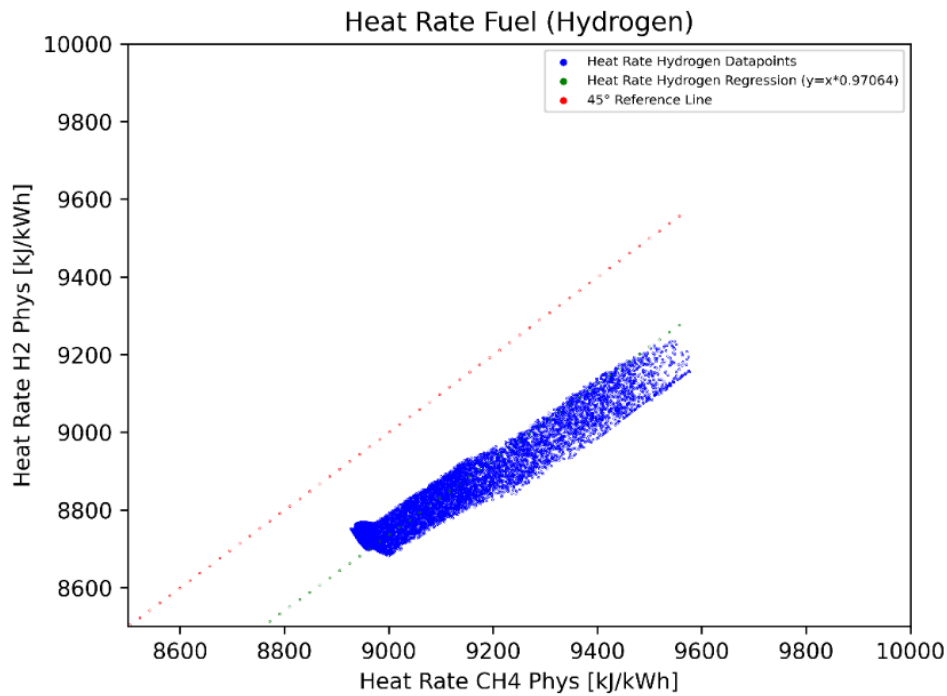
6. Result discussion

As mentioned in the results, the electrical power generated rises when switching from methane to hydrogen. This is true for every scenario calculated. This is especially interesting when looking at the turbines isentropic efficiency for both runs. The reason for this is that the turbine efficiency tends to be lower for the Hydrogen run.



6-1: Isentropic turbine efficiencies for methane and hydrogen

One unexpected aspect of this lower turbine efficiency is that the heat rate also tends to be lower for the hydrogen-fired run. The heat rate is defined as the generated electrical energy of the turbine divided by the supplied energy. Therefore a lower heat rate indicates a higher efficiency [24]. As a result, the whole turbine worked more efficiently when fired with hydrogen, even though the turbines isentropic efficiency was lower.

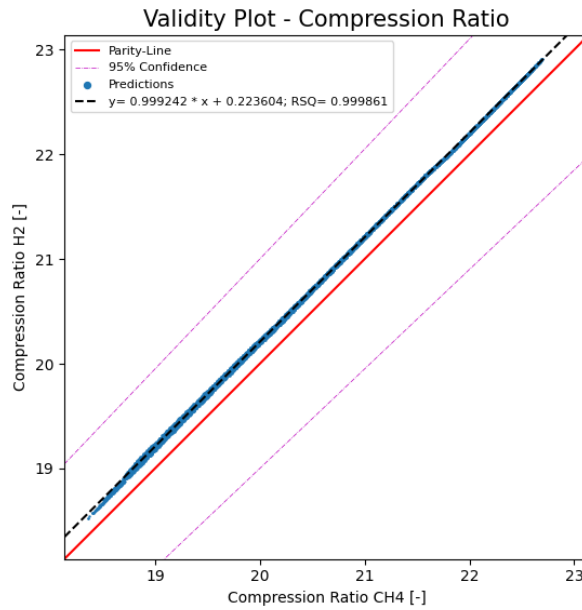


6-2: Heat rates for both runs

Therefore, even though the turbines isentropic efficiency is lower for the Hydrogen Run the overall efficiency tends to be higher. As shown earlier, the thermal efficiency of the cycle is only dependent on the pressure ratio. In the following equation p_1 is the inlet pressure at the compressor and p_2 is the outlet pressure level [17].

$$\eta_{th} = 1 - \left(\frac{p_2}{p_1}\right)^{\frac{(\gamma-1)}{\gamma}} \quad (6-1)$$

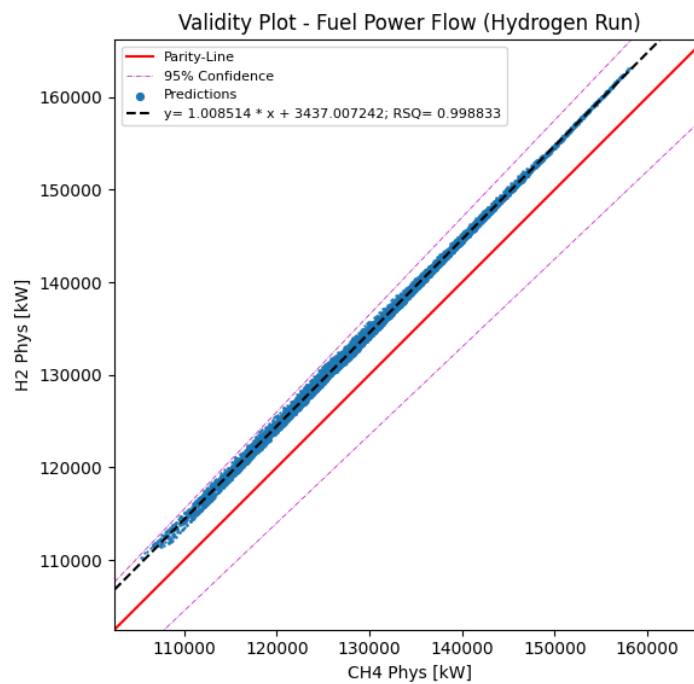
This shows that the theoretical turbine cycle efficiency will rise if the compression ratio rises too. Therefore one possible cause of this turbine behavior is that the pressure level was higher in the Hydrogen Run compared to the Validation Run.



6-3: Compression Ratio Comparison

As can be seen in the plot, this is exactly what happened. The pressure level tends to be higher for the Hydrogen Run resulting in higher cycle efficiency. This can explain why the overall efficiency of the turbine rises, even though the isentropic efficiency of the turbine itself declines.

One possible explanation for the lower isentropic efficiency of the Hydrogen Run is that the fuel power consumption is higher than in the Validation Run. This is shown in the following plot.

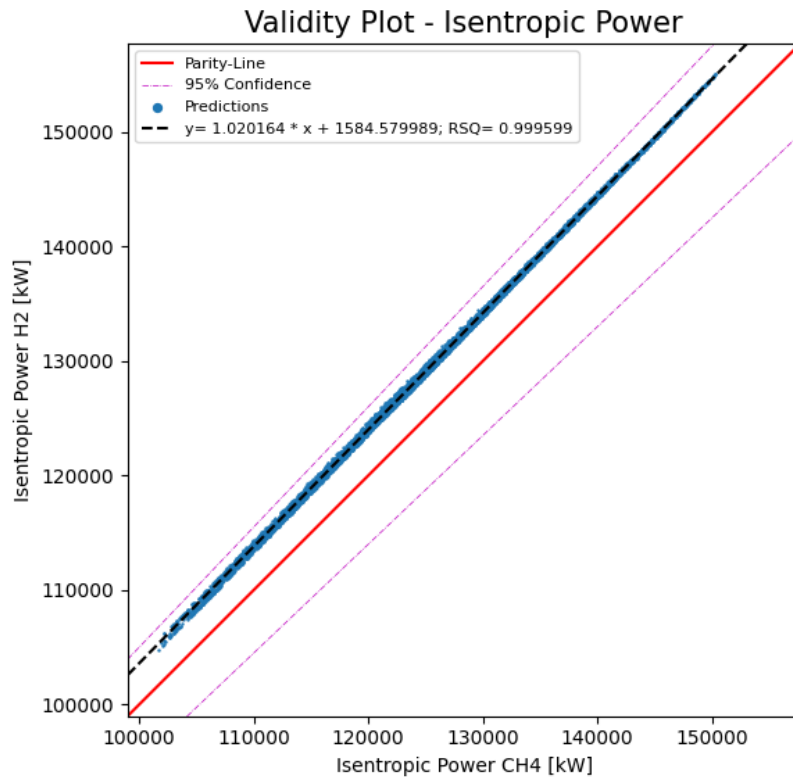


6-4: Comparison of the fuel consumption

This results in a higher firing temperature. This higher temperature also occurs on the turbine inlet. Since the temperature is higher, the isentropic power also rises. A rise in the isentropic power does not mean that the isentropic efficiency has to rise. The isentropic efficiency is defined as follows [37].

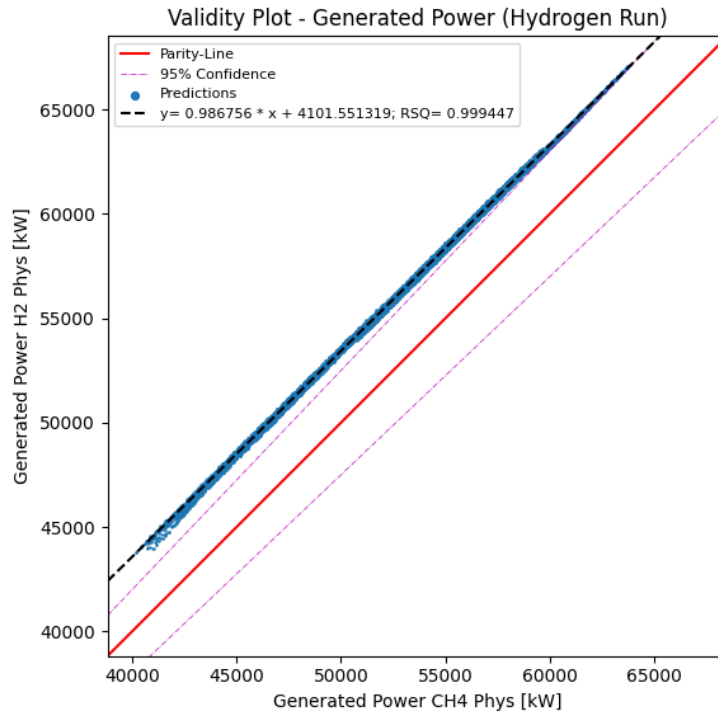
$$\eta_{is} = \frac{\dot{W}_{real}}{\dot{W}_{is}} \quad (6-2)$$

If the isentropic power \dot{W}_{is} rises stronger than the actual power generated by the turbine \dot{W}_{real} , the isentropic efficiency may decline, although the power generated by the turbine rises. The following plot shows the isentropic power of the Hydrogen Run compared to the isentropic power of the Validation Run.



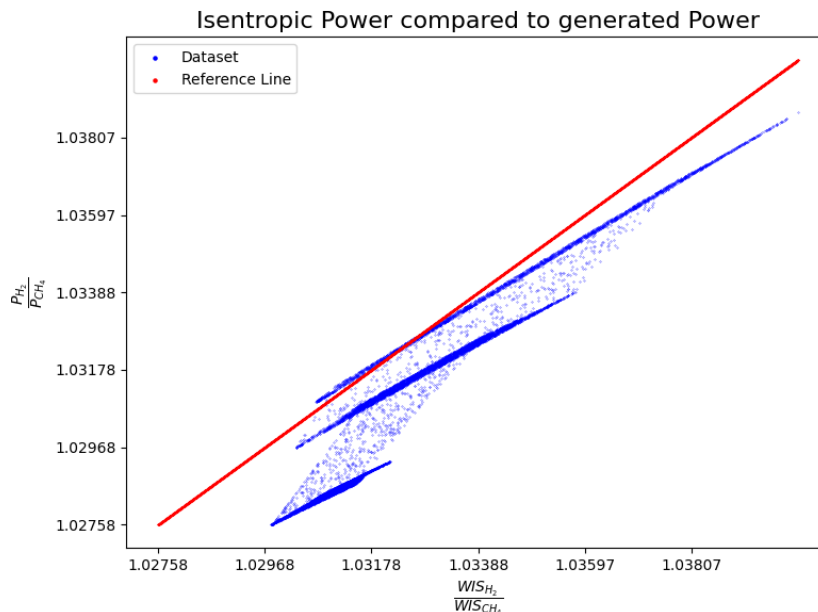
6-5: Comparison of the isentropic power for different fuels

In this plot, it is possible to see that the isentropic power for the Hydrogen Run is higher compared to the Validation Run. This was expected because the Hydrogen Run used to have a higher firing temperature therefore a higher isentropic power was expected. The following plot shows the power generated by the turbine for both runs.



6-6: Comparison of the generated power for different fuels

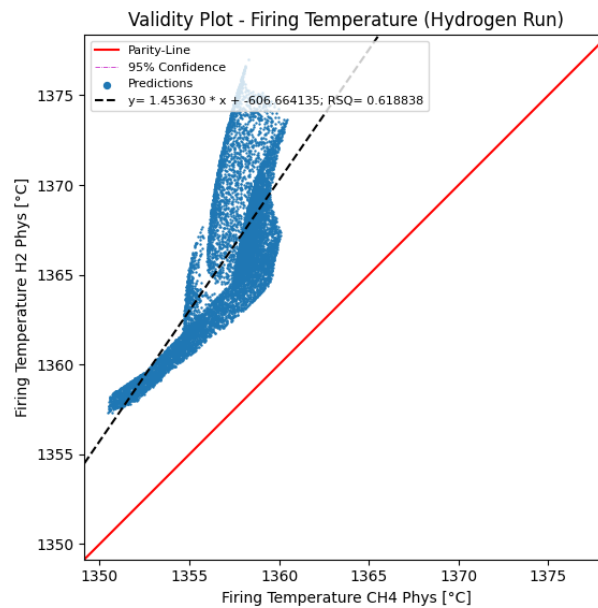
This also shows that the turbine's real generated power is higher for the Hydrogen Run. Since the isentropic power was also higher, this is not unexpected behavior. Therefore the only reason why the turbine efficiency of the Hydrogen Runs could be lower compared to the Validation Run would be if the rise in the real generated power is lower compared to the rise of the isentropic power. In the next plot, the Hydrogen Run's actual power is divided by the generated power of the Validation Run. The same happens to the isentropic power.



6-7: Comparison between the isentropic power and the generated power for different fuels

This plot shows that the rise of the isentropic power is higher than the generated power's rise. Therefore, it can be said that the cycle efficiency of the hydrogen-fired turbine rises compared to the methane-fired one, even though the turbine efficiency tends to be lower.

Another aspect is the firing temperature. While the firing temperature of the Validation Run was very close compared to the Reference Run this is not true for the Hydrogen Run. The firing temperature can be seen in the following plot.



6-8: Firing temperature for different fuels

This diagram shows that the hydrogen-fueled gas turbine's firing temperature was much higher than the methane-fueled one. This also results in the higher power generation of the turbine, as seen in plot 6-8. The problem with this rise in firing temperature is that it is unclear if a real gas turbine could withstand this additional thermal load. If not, this could cause severe damage to the gas turbine. Since the heat supply was too high for hydrogen, the fuel control system did not work as expected. One reason for this behavior is that the flue gas composition changes with a fuel change. This has two significant side effects.

One of these side effects is that the heat intake changes for a given maximal firing temperature. The reason for this is that the heat capacity of the flue gas changes because of the different compositions. Since the flue gas of a hydrogen-fueled gas turbine has a much higher water mass fraction than the methane-fueled one.

Another side effect is that this deviation in the fuel composition also influences the expansion of the flue gas in the turbine. A fuel gas based on hydrogen combustion tends to expand to a lower temperature level than a methane-based one. Since the fuel system regulates the fuel based on the exit temperature, the heat intake tends to be higher compared to a methane-based one.

7. Conclusion

Two conclusions can be drawn based on the interpretation of the results. The first one is that a fuel system that uses the turbine's exhaust temperature to regulate the heat supply will result in higher firing temperatures for hydrogen. This is because a flue gas based on hydrogen combustion expands to a lower exhaust temperature. This is also true if the inlet temperature of the turbine is the same. This behavior will cause the fuel system to raise the exhaust temperature and, therefore the firing temperature. In this case, a methane turbine would be perfectly fine, because this measuring intervention does not exceed the firing temperature to a dangerous level. This is not true for hydrogen-fired gas turbines that will exceed these limits.

For future research, it would be reasonable to investigate the fuel control system even more. In this thesis, one approach was found to model the behavior of a methane-fired gas turbine with great accuracy. This thesis had the underlying assumption that the behavioral differences between methane-fueled and hydrogen-fueled turbines are neglectable for the heat supply. This resulted in a not ideal fuel regulation for hydrogen. The created physical model of the gas turbine SGT-800 (57 MW) is a good starting point for this further investigation of the fuel control system.

8. Bibliography

- [1] *State of the Union 2020 : EU climate target plan 2030 : building a modern, sustainable and resilient Europe*. Luxembourg : Publications Office of the European Union, 2020
- [2] *Trends and projections in Europe*. Luxembourg : Publications Office of the European Union, 2021 (EEA report no 2021, 13)
- [3] POULLIKKAS, Andreas: *An overview of current and future sustainable gas turbine technologies*. In: *Renewable and Sustainable Energy Reviews* 9 (2005), Nr. 5, S. 409–443
- [4] ABUDU, Kamal ; IGIE, Uyioghosa ; MINERVINO, Orlando ; HAMILTON, Richard: *Gas turbine efficiency and ramp rate improvement through compressed air injection*. In: *Proceedings of the Institution of Mechanical Engineers, Part A: Journal of Power and Energy* 235 (2021), Nr. 4, S. 866–884
- [5] PARK, Young-Kwang ; MOON, Seong-Won ; KIM, Tong-Seop: *Advanced Control to Improve the Ramp-Rate of a Gas Turbine: Optimization of Control Schedule*. In: *Energies* 14 (2021), Nr. 23, S. 8024
- [6] FARHAT, Hiyam ; SALVINI, Coriolano: *Novel Gas Turbine Challenges to Support the Clean Energy Transition*. In: *Energies* 15 (2022), Nr. 15, S. 5474
- [7] GAHLEITNER, Gerda: *Hydrogen from renewable electricity: An international review of power-to-gas pilot plants for stationary applications*. In: *International Journal of Hydrogen Energy* 38 (2013), Nr. 5, S. 2039–2061
- [8] FELSEGHI, Raluca-Andreea ; CARCADEA, Elena ; RABOACA, Maria Simona ; TRUFIN, Cătălin Nicolae ; FILOTE, Constantin: *Hydrogen Fuel Cell Technology for the Sustainable Future of Stationary Applications*. In: *Energies* 12 (2019), Nr. 23, S. 4593
- [9] KWON, Hyun Min ; KIM, Tong Seop ; SOHN, Jeong Lak ; KANG, Do Won: *Performance improvement of gas turbine combined cycle power plant by dual cooling of the inlet air and turbine coolant using an absorption chiller*. In: *Energy* 163 (2018), S. 1050–1061
- [10] GLOBAL ENERGY MONITOR: *Globale Energy Monitor's Europe Gas Tracker*. URL <https://globalenergymonitor.org/projects/europe-gas-tracker/tracker-map/>
- [11] VOLPONI, Allan J.: *Gas Turbine Parameter Corrections*. Cham : Springer International Publishing, 2020
- [12] *Ebsilon Professional* : STEAG Energy Services GmbH, 2022. URL <https://www.ebsilon.com/de/>

- [13] SARAVANAMUTTOO, Herbert I. H. ; ROGERS, Gordon F. C. ; COHEN, Henry ; STRAZNICKY, Paul ; NIX, Andrew: *Gas turbine theory*. 7th edition. Harlow, New York, Toronto : Pearson, 2017
- [14] KURZ, Rainer ; BRUN, Klaus: *Gas Turbine Performance*. 2016
- [15] SCHOBEIRI, Meinhard T.: *Turbomachinery Flow Physics and Dynamic Performance*. Berlin, Heidelberg : Springer Berlin Heidelberg, 2012
- [16] ZAHORANSKY, Richard ; ALLELEIN, Hans-Josef ; BOLLIN, Elmar ; OEHLER, Helmut ; SCHELLING, Udo ; SCHWARZ, Harald: *Energietechnik*. Wiesbaden : Springer Fachmedien Wiesbaden, 2013
- [17] BORGNACKE, Claus ; SONNTAG, Richard Edwin: *Fundamentals of thermodynamics*. 8. ed. Hoboken, NJ : Wiley, 2013
- [18] GUHA, A.: *Performance and optimization of gas turbines with real gas effects*. In: *Proceedings of the Institution of Mechanical Engineers, Part A: Journal of Power and Energy* 215 (2001), Nr. 4, S. 507–512
- [19] DOERING, Ernst ; SCHEDWILL, Herbert ; DEHLI, Martin: *Grundlagen der Technischen Thermodynamik : Lehrbuch für Studierende der Ingenieurwissenschaften*. 7., erw. u. überarb. Aufl. 2012. Wiesbaden : Vieweg+Teubner Verlag, 2012 (SpringerLink Bücher)
- [20] GÜLEN, S. Can: *Gas Turbine Combined Cycle Power Plants*. Milton : Taylor & Francis Group, 2020
- [21] KANG, Do Won ; KIM, Tong Seop: *Model-based performance diagnostics of heavy-duty gas turbines using compressor map adaptation*. In: *Applied Energy* 212 (2018), S. 1345–1359
- [22] RAJPUT, R. K.: *Engineering Thermodynamics : [For Engineering Students of All Indian Universities and Competitive Examinations]*. 3rd ed. New Delhi, Boston, USA : Laxmi Publications, 2007
- [23] DICK, Erik: *Fundamentals of Turbomachines*. 2nd ed. 2022. Cham : Springer International Publishing; Imprint Springer, 2022 (Springer eBook Collection 130)
- [24] BOYCE, Meherwan P.: *Gas turbine engineering handbook*. 4th ed. Oxford : Butterworth-Heinemann, 2011
- [25] BAR-MEIR, Genick: *Fundamentals of Compressible Fluid Mechanics* : Zenodo, 2022
- [26] HUTTER, Kolumban ; WANG, Yongqi ; CHUBARENKO, Irina P.: *Dimensional Analysis, Similitude and Model Experiments*. In: HUTTER, Kolumban; CHUBARENKO, Irina P.; WANG,

- Yongqi (Hrsg.): *Physics of Lakes*. Cham : Springer International Publishing, 2014
(Advances in Geophysical and Environmental Mechanics and Mathematics), S. 307–396
- [27] ÇENGEL, Yunus A. ; CIMBALA, John M.: *Fluid mechanics : Fundamentals and applications*.
3rd edition. New York, NY : McGraw-Hill, 2014
- [28] DIXON, Sydney Lawrence ; HALL, Cesare A.: *Fluid mechanics and thermodynamics of turbomachinery*. Seventh edition. Oxford : Butterworth-Heinemann, 2013
- [29] *Volume 1: Aircraft Engine; Ceramics; Coal, Biomass and Alternative Fuels; Manufacturing, Materials and Metallurgy; Microturbines and Small Turbomachinery* :
ASMEDC, 2008
- [30] BÖCKH, Peter von (Hrsg.); SAUMWEBER, Christian (Hrsg.): *Fluidmechanik*. Berlin, Heidelberg
: Springer Berlin Heidelberg, 2013
- [31] BAR-MEIR, Genick: *Fundamentals of Compressible Fluid Mechanics* : Zenodo, 2021
- [32] KAIKKO, Juha: *Performance prediction of gas turbines by solving a system of non-linear equations*. Zugl.: Lappeenranta, University of Technology, Diss., 1998. Lappeenranta,
1998 (Tieteellisiä Julkaisuja / Lappeenrantaan Teknillinen Korkeakoulu 68)
- [33] ALBERTO MISTÉ, Gianluigi ; BENINI, Ernesto: *Turbojet Engine Performance Tuning With a New Map Adaptation Concept*. In: *Journal of Engineering for Gas Turbines and Power*
136 (2014), Nr. 7
- [34] LIU, Zuming ; KARIMI, Iftekhhar A.: *Gas turbine performance prediction via machine learning*. In: *Energy* 192 (2020), S. 116627
- [35] SIEMENS AG: *Siemens gas turbine portfolio*. URL
<https://assets.new.siemens.com/siemens/assets/api/uuid:ab8578bf-d86f-45d9-a26b-7ac7a274fadd/siemens-gas-turbine-portfolio.pdf>
- [36] ETN: *SGT-800 - ETN*. URL <https://etn.global/gas-turbine-products/sgt-800/>. –
Aktualisierungsdatum: 2019-01-16 – Überprüfungsdatum 2022-09-05
- [37] YANG, Bei ; FANG, Xiande ; ZHANG, Lisheng ; ZHUANG, Fengting ; Bi, Minghua ; CHEN, Chuang
; LI, Gen ; WANG, Xi: *Applicability of empirical models of isentropic efficiency and mass flow rate of dynamic compressors to jet engines*. In: *Progress in Aerospace Sciences* 106
(2019), S. 32–42
- [38] MALLINSON, D. H. ; LEWIS, W. G. E.: *The Part-Load Performance of Various Gas-Turbine Engine Schemes*. In: *Proceedings of the Institution of Mechanical Engineers* 159 (1948),
Nr. 1, S. 198–219

- [39] FULS, W. F.: *Enhancement to the Traditional Ellipse Law for More Accurate Modeling of a Turbine With a Finite Number of Stages*. In: *Journal of Engineering for Gas Turbines and Power* 139 (2017), Nr. 11
- [40] PETROVIC, Milan V. ; WIEDERMANN, Alexander: *Through-Flow Analysis of Air-Cooled Gas Turbines*. In: *Journal of Turbomachinery* 135 (2013), Nr. 6
- [41] *Volume 3: Turbo Expo 2007* : ASME/EDC, 2007
- [42] KHAN, Arshad: *Technical and financial analysis of combined cycle gas turbine*. In: *Thermal Science* 17 (2013), Nr. 3, S. 931–942
- [43] BAAKEEM, Saleh ; ORFI, Jamel ; ALAQEL, Shaker ; AL-ANSARY, Hany: *Impact of Ambient Conditions of Arab Gulf Countries on the Performance of Gas Turbines Using Energy and Exergy Analysis*. In: *Entropy* 19 (2017), Nr. 1, S. 32
- [44] FREUND, Rudolf J. ; WILSON, William J. ; SA, Ping: *Regression Analysis*. 2. Aufl. s.l. : Elsevier professional, 2006
- [45] ÜBERHUBER, Christoph: *Computer-Numerik 1*. Berlin : Springer, 1995